



Calhoun: The NPS Institutional Archive
DSpace Repository

Theses and Dissertations

1. Thesis and Dissertation Collection, all items

1990-09

Vibration of a cantilever beam that slides axially in a rigid frictionless hole

DeVries, Mark R.

Monterey, California: Naval Postgraduate School

<http://hdl.handle.net/10945/34883>

This publication is a work of the U.S. Government as defined in Title 17, United States Code, Section 101. Copyright protection is not available for this work in the United States.

Downloaded from NPS Archive: Calhoun



Calhoun is the Naval Postgraduate School's public access digital repository for research materials and institutional publications created by the NPS community. Calhoun is named for Professor of Mathematics Guy K. Calhoun, NPS's first appointed -- and published -- scholarly author.

Dudley Knox Library / Naval Postgraduate School
411 Dyer Road / 1 University Circle
Monterey, California USA 93943

<http://www.nps.edu/library>

(2)

NAVAL POSTGRADUATE SCHOOL Monterey, California

AD-A241 352



DTIC
ELECTE
OCT 08 1991
S B D

THESIS

VIBRATION OF A CANTILEVER BEAM
THAT SLIDES AXIALLY
IN A RIGID FRICTIONLESS HOLE

by

Mark R. DeVries

September, 1990

Thesis Advisor:

David Salinas

Approved for public release; distribution is unlimited.

91-12524



UNCLASSIFIED

SECURITY CLASSIFICATION OF THIS PAGE

REPORT DOCUMENTATION PAGE				
1a REPORT SECURITY CLASSIFICATION UNCLASSIFIED			1b RESTRICTIVE MARKINGS NONE	
2a SECURITY CLASSIFICATION AUTHORITY			3 DISTRIBUTION/AVAILABILITY OF REPORT Approved for public release; distribution is unlimited.	
2b DECLASSIFICATION/DOWNGRADING SCHEDULE				
4 PERFORMING ORGANIZATION REPORT NUMBER(S)			5 MONITORING ORGANIZATION REPORT NUMBER(S)	
6a NAME OF PERFORMING ORGANIZATION Naval Postgraduate School		6b OFFICE SYMBOL (If applicable) 069	7a NAME OF MONITORING ORGANIZATION Naval Postgraduate School	
6c ADDRESS (City, State, and ZIP Code) Monterey, CA 93943-5000			7b ADDRESS (City, State, and ZIP Code) Monterey, CA 93943-5000	
8a NAME OF FUNDING/SPONSORING ORGANIZATION		8b OFFICE SYMBOL (If applicable)	9 PROCUREMENT INSTRUMENT IDENTIFICATION NUMBER	
8c ADDRESS (City, State, and ZIP Code)			10 SOURCE OF FUNDING NUMBERS	
			Program Element No.	Project No.
			Task No.	Work Unit Accession Number
11 TITLE (Include Security Classification) VIBRATION OF A CANTILEVER BEAM THAT SLIDES AXIALLY IN A RIGID FRICTIONLESS HOLE				
12 PERSONAL AUTHOR(S) DEVRIES, MARK R.				
13a TYPE OF REPORT Master's Thesis		13b TIME COVERED From To	14 DATE OF REPORT (year, month, day) 1990 SEPTEMBER	15 PAGE COUNT 124
16 SUPPLEMENTARY NOTATION The views expressed in this thesis are those of the author and do not reflect the official policy or position of the Department of Defense or the U.S. Government.				
17 COSATI CODES			18 SUBJECT TERMS (continue on reverse if necessary and identify by block number)	
FIELD	GROUP	SUBGROUP	Cantilever Beam, Finite Element Method, Axial Motion, Vibration, Transient Behavior	
19 ABSTRACT (continue on reverse if necessary and identify by block number) This research considers a cantilever beam which can move axially in and out of a rigid frictionless hole and is free to vibrate laterally outside the hole. Two Euler equations describing the lateral and axial motion of the beam are presented. A transformation of coordinates to eliminate the moving boundary, and spatial non dimensionalization are used to transform the problem into a system of two coupled non linear partial differential equations with a fixed domain. A finite element formulation provides a numerical solution to the problem. Results for some problems are presented.				
20 DISTRIBUTION/AVAILABILITY OF ABSTRACT <input checked="" type="checkbox"/> UNCLASSIFIED FOR PUBLIC RELEASE <input type="checkbox"/> SAME AS REPORT <input type="checkbox"/> RESTRICTED			21 ABSTRACT SECURITY CLASSIFICATION UNCLASSIFIED	
22a NAME OF RESPONSIBLE INDIVIDUAL DAVID SALINAS			22b TELEPHONE (Include Area code) (408) 646 3426	22c OFFICE SYMBOL Code 69Sa

DD FORM 1473, 84 MAR

83 APR edition may be used until exhausted
All other editions are obsolete

SECURITY CLASSIFICATION OF THIS PAGE

UNCLASSIFIED

Approved for public release; distribution is unlimited.

Vibration of a Cantilever Beam
that Slides Axially in a
Rigid Frictionless Hole

by

Mark R. DeVries
Lieutenant, United States Coast Guard
B.S., United States Coast Guard Academy, 1981

Submitted in partial fulfillment
of the requirements for the degree of

MASTER OF SCIENCE IN MECHANICAL ENGINEERING

from the


NAVAL POSTGRADUATE SCHOOL
September 1990

Author:


Mark R. DeVries

Approved by:


David Salinas, Thesis Advisor


Anthony J. Healy, Chairman
Department of Mechanical Engineering

ABSTRACT

This research considers a cantilever beam which can move axially in and out of a rigid frictionless hole and is free to vibrate laterally outside the hole. Two Euler equations describing the lateral and axial motion of the beam are presented. A transformation of coordinates to eliminate the moving boundary, and spatial non dimensionalization are used to transform the problem into a system of two coupled non linear partial differential equations with a fixed domain. A finite element formulation provides a numerical solution to the problem. Results for some problems are presented.



Accession For	
NTIS GRA&I	<input checked="checked" type="checkbox"/>
DTIC TAB	<input type="checkbox"/>
Unannounced	<input type="checkbox"/>
Justification	
By	
Distribution/	
Availability Codes	
Dist	Avail and/or Special
A-1	

TABLE OF CONTENTS

I. INTRODUCTION	1
II. PROBLEM FORMULATION	4
A. THE EULER EQUATION OF LATERAL MOTION	6
B. THE EULER EQUATION OF AXIAL MOTION	8
C. THE MOVING BOUNDARY	9
D. THE COORDINATE TRANSFORMATION	10
1. Transformation of the Spatial Fourth Derivative of v	11
2. Transformation of the Time Second Derivative of v	12
E. THE FINAL EULER EQUATIONS	15
1. The Transformed Euler Equation for Lateral Deflection	15
2. The Transformed Euler Equation for Axial Motion	16
3. Non dimensionalization of the Lateral Deflection, v	17
a. Final Euler Equation of Lateral Motion .	19
b. Final Euler Equation of Axial Motion . .	20
F. CASES	20

1. Case One, $L(t)$ Prescribed	21
2. Case Two, $F(t)$ Prescribed	21
III. SOLUTION METHOD	25
A. FINITE ELEMENT METHOD DEVELOPMENT	25
1. Construction of the Beam Element	25
2. Global FEM Formulation	27
3. Galerkin FEM Formulation	29
4. Integration of the Galerkin Equation	33
a. Reduction of the Second Order System	33
b. Boundary and Initial Conditions	36
B. FEM VERIFICATION	40
C. THE $F(t)$ PRESCRIBED SOLUTION METHOD	47
IV. CASE STUDY REPORT AND CONCLUSIONS	52
A. GENERAL DISCUSSION	52
1. Time Step Convergence	53
2. Spatial Grid Convergence	54
3. Computational Effort	55
4. The Case Study Beam	56
B. FIRST CASE STUDY, NEGLIGIBLE DERIVATIVES OF $L(t)$	57
C. SECOND CASE STUDY, PARABOLIC FUNCTIONS OF $L(t)$	61
1. Parabolic $L(t)$, The Less Stiff Beam	62
2. Parabolic $L(t)$, The Stiff Beam	64
3. Discussion of the Parabolic Cases	66
D. HARMONIC $L(t)$ PRESCRIBED	67

E. CASE STUDY FOUR, TRACKING WORK FOR A PARABOLIC PRESCRIBED $L(t)$	70
F. FINAL COMMENTS AND RECOMMENDATIONS	73
APPENDIX A THE CUBIC SPLINE SHAPE FUNCTIONS	87
APPENDIX B CONSTRUCTION OF THE GLOBAL MATRICES	90
APPENDIX C STATIC CANTILEVER BEAM FORTRAN CODE	94
APPENDIX D INTEGRATION BY PARTS	100
APPENDIX E TRANSIENT BEHAVIOR OF A CANTILEVER BEAM FORTRAN CODE	102
LIST OF REFERENCES	110
INITIAL DISTRIBUTION LIST	111

LIST OF FIGURES

2.1	Cantilever Beam Moving Axially in a Frictionless Hole	5
2.2	Region of Integration for Equation (1)	9
2.3	Region of Integration for Equation (25)	10
4.1	Beam Geometry	57
4.2	Parabolic and Linear Initial Conditions Plot Case Study One and Four	59
4.3	Length and Velocity Function Plots Case Study One	60
4.4	Parabolic and Linear Initial Conditions Plot Case Study Two	62
4.5	Length, Velocity, and Acceleration Function Plots Case Study Two (Less Stiff Beam)	63
4.6	Length, Velocity, and Acceleration Function Plots Case Study Two (Stiff Beam)	65
4.7	Length, Velocity, and Acceleration Function Plots Case Study Three (Both Beams)	68
4.8	Sinusoidal Initial Conditions Plot	69
4.9	Length, Velocity, and Acceleration Function Plots Case Study Four	71
4.10	Parabolic Axial Motion Transient Response Case Study Two (Stiff Beam)	75
4.11	Parabolic Axial Motion Transient Response Case Study Two (Less Stiff Beam)	76
4.12	Harmonic Axial Motion Transient Response Case Study Three (Stiff Beam)	77
4.13	Harmonic Axial Motion Transient Response Case Study Three (Less Stiff Beam)	78

4.14	Parabolic Axial Motion Transient Response Case Study Four	79
4.15	Shear Plot (0.0 - 1.0 Seconds)	80
4.16	Shear Plot (1.0 - 2.0 Seconds)	81
4.17	Shear Plot (2.0 - 3.0 Seconds)	82
4.18	Moment Plot (0.0 - 1.0 Seconds)	83
4.19	Moment Plot (1.0 - 2.0 Seconds)	84
4.20	Moment Plot (2.0 - 3.0 Seconds)	85
4.21	Force and Work Plots Case Four	86
A.1	Cubic Spline Shape Functions	87
B.1	Transformation from the global ξ coordinate to the local α coordinate	91

LIST OF SYMBOLS

A, B, C, D	2nd order system finite element operator matrices
$B.T.$	Boundary term vector
C_i	Linearization terms
DOF	Degrees of freedom
E	Young's modulus of elasticity
$F(t)$	Axial force as a function of time
F, K, M, P	Matrices of convenience (multiples and summations of previously defined variables and matrices)
G, H, Ω	1st order system finite element operator matrices
I	Moment of inertia of the beam cross-section
J_i	Collection of terms assigned values from previous integration
L_0	Initial length of beam
$L(t)$	Instantaneous length of beam
q	Substitution variable, $q = L$
M	Applied moment
N	Number of elements
\bar{N}	Number of DOF
p	Internally applied load
p^*	Non dimensional internal loading
P	Applied load
q_i	Set of cubic spline shape functions
Q	Vector of finite element global shape functions

R	Residual function
t	Time
u'	Axial deformation
$u(t)$	Axial motion as a function of time
β	Material and geometric properties variable
δ	2nd order system global DOF, system solution set
η	Transformation coordinate for time
θ	Slope
λ	1st order system global DOF, system solution set
λ_0	Vector of initial conditions for all DOF
v^*	Non dimensional lateral motion
$v(t)$	Lateral Motion as a function of time and axial position
ξ	Non dimensional coordinate in the axial direction
ρ	Mass of the beam per unit length
ω	Substitution vector, $\omega = \delta$

ACKNOWLEDGEMENTS

The author would like to express his deep appreciation to Professor David Salinas for his guidance, patience, dedication, friendship, and "open door". The author also wishes to recognize and thank Jeffre Simmen, who always made himself available to assist and discuss various mathematical elements of the problem. Finally, the author greatly appreciates the assistance rendered by Richard Donat, Roger Hilleary, and Dennis Mar of the Naval Postgraduate School Computer Center. To all of you who have made this such an enjoyable and memorable experience, please accept this expression of my gratitude.

I. INTRODUCTION

A literature search of the engineering journals shows that an investigation of the transient behavior of a cantilever beam, free to move axially in a frictionless hole at its 'fixed' end, has not been undertaken to this date. In 1979, Boresi and Salinas prepared a report for the Naval Sea Systems Command, that formulates the problem and proposes a solution procedure. The report was the result of an interest in the transient behavior of a gun barrel during recoil following firing. [Ref.1]

Hamilton's principle was used to generate the governing partial differential equations for axial and lateral motion of the beam [Ref.1]. As a result of axial motion of the beam, the length of the beam changes with time. Thus the 'free' end of the cantilever beam is a moving boundary point. If the beam is subjected to an axial force, then the beam length, that is the location of the 'free' end, is an unknown which is itself a solution of the problem. This is a 'conjugate' problem, wherein the boundary condition is a solution of a problem which can not be solved until the boundary extent is known. The analogy is of a dog chasing its own tail, or the 'catch 22' syndrome. The dilemma is resolved by introducing a coordinate transformation which produces a classical two-point (fixed) boundary domain. The removal of the moving

boundary is not without expense, as the resulting governing partial differential equations are significantly more complicated. Thus the complication of the boundary condition has been 'transferred' into the interior domain of the problem. The two equations governing axial and lateral motion, for beam length and lateral motion, are both coupled and nonlinear if the axial motion is not prescribed.

Using the finite element method over the spatial domain, the two partial differential equations in space and time, are reduced to a system of ordinary differential equations in time only. That is, the original initial-(two-point) boundary value problem is transformed into a system of initial-value problems for the transient behavior at discrete points of the system. These nonlinear O.D.E.'s are linearized using the quasi-linearization technique of Bellman [Ref.2], and then solved by using a fifth order Gear' method for stiff equations

This investigation adds further to the formulation of the problem by the introduction of non dimensional variables. Additionally, the work also provides mathematical development and details required for the numerical solution of the problem. Restrictions and a generalization of the problem are also discussed.

The scope of the problem suggests a cautious two-stage investigation. In the first stage, the axial motion as a function of time is prescribed. The result is the elimination of the need to solve the equation for axial motion. However,

the equation can be used to solve for the axial force directly. Moreover, the remaining governing equation for lateral transient behavior is linear since the 'length' term in the equation is known. It is felt that the first stage investigation, which is the body of this thesis activity, would provide useful insight into the nature of the problem prior to undertaking the second stage investigation. In the second stage investigation, instead of prescribing the axial motion, the axial force at the sliding end is prescribed. As a result, the equation for the transient axial response needs to be solved in conjunction with the equation for transient lateral response, since now the length of the beam is also unknown. The second stage problem is formulated but not solved here.

II. PROBLEM FORMULATION

Consider the transient behavior of a cantilever beam fitted snugly into a frictionless hole as shown in Figure (2.1). The beam is free to move axially and laterally when an axial force $F(t)$ is applied, or when otherwise an axial displacement is imposed. The beam's motion can be defined completely by its axial motion $u(t)$ as a function of time, and its lateral motion $v(x,t)$ as a function of both time and position along the x axis. Because of inertia, under certain conditions, such as when the axial force $F(t)$ is a large magnitude impulse, the axial movement of the beam may tend to bend the beam by beam-column action or compress the beam axially by beam-bar action. These axial deformation effects are not considered here, that is $u' = 0$. Therefore, it is assumed that all points along the x -axis of the beam experience the same axial motion. Thus, the instantaneous length of the beam, $L(t)$, serves to describe the axial motion of all points of the beam.

As the beam moves axially, the length of the beam outside the hole at any time t is defined as $L(t)$. Because $L(t)$ is changing with time the extent of the domain of the problem changes with time. It is this changing domain that results in the coupling of the equations which describe the lateral and

axial motion of the beam. The changing domain is the essence of the problem and will be discussed at length in the development that follows. This investigation will be restricted to long slender beams, which in this case will be beams for which the length is equal to or greater than ten times either of the cross-sectional dimensions. With this restriction imposed, the Timoshenko Beam shear effects and rotary inertia, are neglected [Ref. 3]. However, as the beam length becomes shorter these effects become larger and loss of accuracy in the solution is expected.

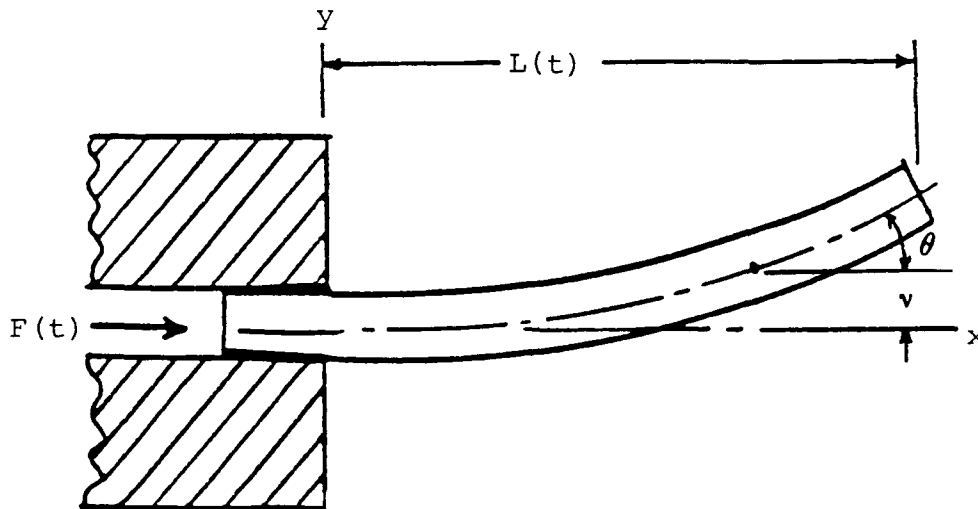


Figure 2.1 Cantilever Beam Moving Axially in a Frictionless Hole

A. THE EULER EQUATION OF LATERAL MOTION

Imposing equilibrium in the lateral direction and using small displacement theory results in the Euler Equation for the lateral motion of a beam,

$$\begin{aligned}EI v_{xxxx}(x, t) + \rho v_{tt}(x, t) &= p(x, t) \\ t &> 0 \\ 0 < x < L(t)\end{aligned}\tag{1}$$

where the subscripts t and x denote partial differentiation with respect to time and position, respectively and;

$v(x, t)$ = the lateral displacement as a function of x and t .

E = Young's modulus of elasticity of the beam.

I = moment of inertia of the beam cross-section.

ρ = the mass of the beam per unit length (constant).

P = the internally applied load per unit length.

The fourth order Euler Equation has two essential (forced) boundary conditions on displacement and slope at the 'fixed' left end,

$$\begin{aligned}v(0, t) &= 0 \\ v_x(0, t) &= 0\end{aligned}\tag{2}$$

and two natural boundary conditions on moment and shear force at the 'free' right end,

$$\begin{aligned}EI v_{xx}(L, t) &= M \\EI v_{xxx}(L, t) &= P\end{aligned}\tag{3}$$

where M and P are the applied moment and load, respectively. The homogeneous boundary conditions ($M = P = 0$) are the boundary conditions considered here. However, a verification of the solution method is presented where the non homogeneous boundary conditions are imposed. The term 'fixed' end is used in reference to the boundary located at the left end of the beam's domain (See Figure 2.2), i.e., at $x=0$. As a result of the axial motion, the point on the beam at this left or 'fixed' end is changing with time.

The natural boundary conditions at the free end (Eqs. 3), for moment and shear, occurs at the right end point of the beam (i.e., at $x = L$) for all time t . It is the fact that the argument L in Equations (3) is changing with time that makes the natural boundary conditions troublesome. These so called moving boundary conditions (or changing domain) will be discussed later at length.

The Euler Equation for lateral motion is also a second order differential equation in time. To obtain a solution, two initial conditions, one on its lateral position $v(x, 0)$, and one on its velocity $v_t(x, 0)$, along the x axis will be

needed. These initial conditions will depend on the specific problem being solved.

B. THE EULER EQUATION OF AXIAL MOTION

If $F(t)$ rather than $L(t)$ is prescribed, then a differential equation defining $L(t)$ is needed. Again, using principles of equilibrium for motion in the axial direction, the following Euler equation for axial behavior is obtained,

$$\dot{L}(t) + \frac{1}{2\rho L_0} [EI v_{xx}^2(L, t) - \rho v_t^2(L, t)] = \frac{1}{\rho L_0} F(t) \quad (4)$$

Equation (4) is subject to the initial conditions,

$$\begin{aligned} L(0) &= L_0 \\ \dot{L}(0) &= \dot{L}_0 \end{aligned} \quad (5)$$

where L_0 is the initial length of the beam at time $t = 0$. The dot and double dot above L denote the first and second derivatives with respect to time respectively, that is the velocity and acceleration of axial motion.

Together Equations (1) and (4) along with their respective boundary and initial conditions form a coupled and nonlinear, initial-boundary value problem. When the force $F(t)$ is known, these coupled nonlinear equations can be solved using the finite element method with a linearization scheme to find

$v(x,t)$ and $L(t)$. When $L(t)$ is specified, Equation (4) yields $F(t)$ directly.

C. THE MOVING BOUNDARY

In the boundary conditions described in Equations (3), the beam length $L(t)$ is a function of time. Thus the boundary conditions are conditions on a boundary which is moving. Graphically this is shown in Figure (2.2). The curved boundary of the region of integration presents a problem. The desire is to remove the argument of time varying length from the boundary condition at the free end. In essence, we desire to secure the boundary. Graphically the boundary becomes a straight line where previously it was a curved line (See Figure 2.3). This can be achieved by using a coordinate transformation as shown in the next section.

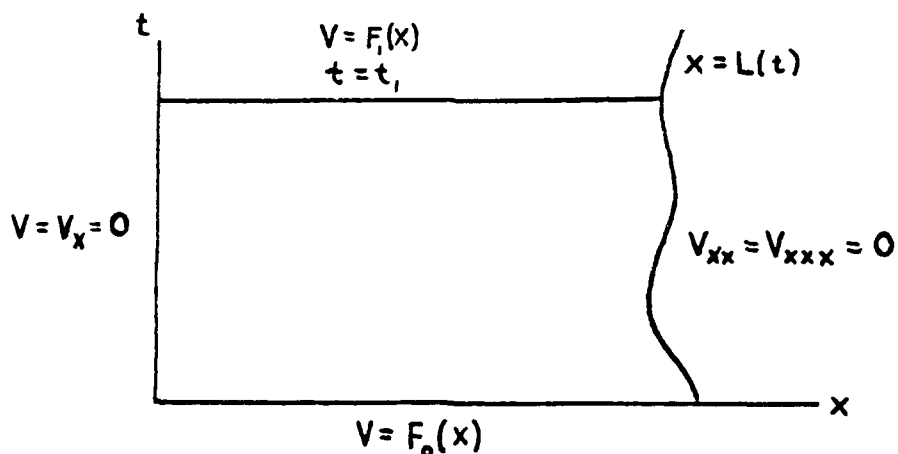


Figure 2.2 Region of Integration for Equation (1)

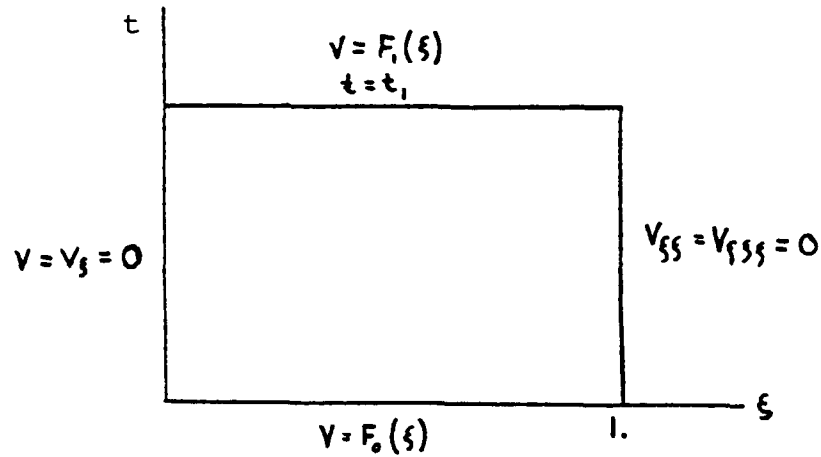


Figure 2.3 Region of Integration for Equation (25)

D. THE COORDINATE TRANSFORMATION

New variables $\xi(x, t)$ and $\eta(t)$ are introduced as follows:

$$\begin{aligned}\xi &= \frac{x}{L(t)} \\ \eta &= t\end{aligned}\tag{6}$$

It should be noted that ξ is a non-dimensional variable with respect to the spatial domain. The lateral deflection now becomes a function of these variables as shown below.

$$\begin{aligned}v(x(\xi, \eta), t(\xi, \eta)) \quad , \text{ or} \\ v(\xi(x, t), \eta(x, t))\end{aligned}\tag{7}$$

Considering the relations defined in Equations (6), the following partial derivatives are obtained.

$$\begin{aligned}
 \frac{\partial \xi}{\partial x} &= \frac{1}{L} \\
 \frac{\partial \xi}{\partial t} &= \frac{-x\dot{L}}{L^2} = \frac{-\xi\dot{L}}{L}, \text{ where } \dot{L} = \frac{\partial L}{\partial t} \\
 \frac{\partial \eta}{\partial t} &= 1 \\
 \frac{\partial \eta}{\partial x} &= 0
 \end{aligned} \tag{8}$$

1. Transformation of the Spatial Fourth Derivative of v

Considering Equation (7), the transformation of the spatial fourth derivative on lateral displacement, v_{xxxx} to the new coordinate ξ is accomplished through a series of differentiations using the chain rule. The first differentiation results in,

$$\frac{\partial v}{\partial x} = \frac{\partial v}{\partial \xi} \frac{\partial \xi}{\partial x} + \frac{\partial v}{\partial \eta} \frac{\partial \eta}{\partial x} \tag{9}$$

Following the substitution of Equations (8) into Equation (9), Equation (10) is obtained.

$$v_x = \frac{1}{L} v_\xi \tag{10}$$

After another differentiation with the chain rule the second spacial derivative is found.

$$\frac{\partial^2 v}{\partial x^2} = \frac{\partial}{\partial x}(v_x) = \frac{\partial}{\partial x}\left(\frac{1}{L}v_\xi\right) = \frac{\partial}{\partial \xi}\left(\frac{1}{L}v_\xi\right)\frac{\partial \xi}{\partial x} + \frac{\partial}{\partial \eta}\left(\frac{1}{L}v_\xi\right)\frac{\partial \eta}{\partial x} \quad (11)$$

Again, using Equations (8), the second derivative is equal to,

$$v_{xx} = \frac{1}{L^2}v_{\xi\xi} \quad (12)$$

Likewise, the third derivative is,

$$v_{xxx} = \frac{1}{L^3}v_{\xi\xi\xi} \quad (13)$$

and finally the fourth derivative is,

$$v_{xxxx} = \frac{1}{L^4}v_{\xi\xi\xi\xi} \quad (14)$$

2. Transformation of the Time Second Derivative of v

The transformation of the time second derivative on lateral deflection (or acceleration), v_{tt} to the new coordinates ξ and η is performed in a similar fashion as was the transformation of it spacial derivatives. Once again,

using Equation (7) and the chain rule, the following expression for the first time derivative is obtained.

$$v_t = \frac{\partial v}{\partial t} = \frac{\partial v}{\partial \xi} \frac{\partial \xi}{\partial t} + \frac{\partial v}{\partial \eta} \frac{\partial \eta}{\partial t} \quad (15)$$

Substituting the Equation (8) values of the partial derivatives into Equation (15) results in the following expression for v_t ,

$$v_t = -\frac{\xi \dot{L}}{L} v_\xi + v_\eta \quad (16)$$

Another time derivative using the chain rule results in the following equation for v_{tt} ,

$$\begin{aligned} v_{tt} &= \frac{\partial}{\partial t} (v_t) \\ &= \frac{\partial}{\partial t} \left[-\frac{\xi \dot{L}}{L} v_\xi + v_\eta \right] \\ &= \frac{\partial}{\partial \xi} \left[-\xi \frac{\dot{L}}{L} v_\xi + v_\eta \right] \frac{\partial \xi}{\partial t} + \frac{\partial}{\partial \eta} \left[-\xi \frac{\dot{L}}{L} v_\xi + v_\eta \right] \frac{\partial \eta}{\partial t} \end{aligned} \quad (17)$$

Again, using Equations (8),

$$\frac{\partial \xi}{\partial t} = -\frac{\xi \dot{L}}{L} \quad \text{and,} \quad \frac{\partial \eta}{\partial t} = 1 \quad (18)$$

along with the product rule of differentiation, we obtain

$$v_{tt} = \left[-\frac{\dot{L}}{L} v_{\xi} - \xi \frac{\dot{L}}{L} v_{\xi\xi} + v_{\xi\eta} \right] \left(-\xi \frac{\dot{L}}{L} \right) + \left[-\xi v_{\xi} \frac{\partial}{\partial \eta} \left(\frac{\dot{L}}{L} \right) \frac{\partial \eta}{\partial t} - \xi \frac{\dot{L}}{L} v_{\xi\eta} + v_{\eta\eta} \right] \quad (19)$$

Recalling that the coordinate transformation on time stated that $t=\eta$, it follows that,

$$\dot{L}(t) = \dot{L}(\eta) = \frac{\partial L}{\partial t} = \frac{\partial L}{\partial \eta} \quad (20)$$

Now, using the quotient rule of differentiation, Equation (19) becomes,

$$v_{tt} = \left[-\frac{\dot{L}}{L} v_{\xi} - \xi \frac{\dot{L}}{L} v_{\xi\xi} + v_{\xi\eta} \right] \left(-\xi \frac{\dot{L}}{L} \right) - \xi v_{\xi} \frac{L\ddot{L} - \dot{L}^2}{L^2} - \xi \frac{\dot{L}}{L} v_{\xi\eta} + v_{\eta\eta} \quad (21)$$

Finally, after multiplying and collecting like terms, v_{tt} becomes,

$$v_{tt} = \xi^2 \frac{\dot{L}^2}{L^2} v_{\xi\xi} + 2\xi \frac{\dot{L}^2}{L^2} v_{\xi} - 2\xi \frac{\dot{L}}{L} v_{\xi\eta} - \xi \frac{\ddot{L}}{L} v_{\xi} + v_{\eta\eta} \quad (22)$$

E. THE FINAL EULER EQUATIONS

Using the transformed operators, the Euler Equations are rewritten in terms of the new coordinates, ξ and η .

1. The Transformed Euler Equation for Lateral Deflection

Substituting the transformed operators from Equations (14) and (22), into the original Euler Equation for lateral deflection,

$$EI v_{xxxx} + \rho v_{tt} = p(x, t) \quad (1)$$

results in the following Euler Equation transformed to the ξ and η coordinates,

$$\frac{EI}{L^4} v_{\xi\xi\xi\xi} + \rho \left[\xi^2 \left(\frac{\dot{L}}{L} \right)^2 v_{\xi\xi} + 2\xi \left(\frac{\dot{L}}{L} \right)^2 v_{\xi} - 2\xi \frac{\dot{L}}{L} v_{\xi\eta} - \xi \frac{\ddot{L}}{L} v_{\xi} + v_{\eta\eta} \right] = p(\xi, \eta)$$

Multiplying through by the inverse of the coefficient of $v_{\xi\xi\xi\xi}$ gives,

$$v_{\xi\xi\xi\xi} + \frac{\rho L^4}{EI} \left[\xi^2 \left(\frac{\dot{L}}{L} \right)^2 v_{\xi\xi} + 2\xi \left(\frac{\dot{L}}{L} \right) \dot{v}_{\xi} - 2\xi \frac{\dot{L}}{L} v_{\xi\eta} - \xi \frac{\ddot{L}}{L} v_{\xi} + v_{\eta\eta} \right] = \frac{L^4}{EI} P(\xi, \eta) \quad (25)$$

$$0 < \xi < 1$$

$$0 < \eta$$

and its boundary conditions,

$$\begin{aligned} v(0, \eta) &= 0 & v_{\xi\xi}(1, \eta) &= 0 \\ v_{\xi}(0, \eta) &= 0 & v_{\xi\xi\xi}(1, \eta) &= 0 \end{aligned} \quad (26)$$

The boundary conditions are now functions of ξ over the domain $0 < \xi < 1$, in lieu of x over the domain $0 < x < L(t)$. The initial conditions on deflection and velocity will be functions of ξ as well.

2. The Transformed Euler Equation for Axial Motion

The coordinate transformation on the Euler Equation of axial motion shown again here,

$$\ddot{L}(t) + \frac{1}{2\rho L_0} [EI v_{xx}^2(L, t) - \rho v_t^2(L, t)] = \frac{1}{\rho L_0} F(t) \quad (4)$$

results in the transformed equation,

$$\ddot{L} + \frac{1}{2\rho L_0} \left(\frac{EI}{L^4} v_{\xi\xi}^2(1, \eta) - \rho \left[-\frac{\dot{L}}{L} v_{\xi}(1, \eta) + v_{\eta}(1, \eta) \right]^2 \right) = \frac{1}{\rho L_0} F(\eta) \quad (28)$$

subjected to the initial conditions in Equations (5).

3. Non dimensionalization of the Lateral Deflection, v

The purpose of the coordinate transformation just completed was to deal with the difficulty presented by the moving boundary condition at the free end of the beam. The four boundary conditions of Equations (2) and (3) were also transformed to the ξ and η coordinates as shown in Equations (26). One of the great difficulties encountered in this investigation resulted from the coordinate transformation performed on the boundary conditions. After the introduction of the non dimensional variable ξ , the finite element method (FEM) of Chapter III was pursued. This included an attempt to confirm the FEM program on a couple of statics problems with known solutions. The resulting FEM solutions were L^3 larger for displacements and L^2 larger for slopes. We had simply imposed the load (or moment) as one would have if the problem had the dimensional independent variable x , when in fact x had been replaced by the non dimensional variable $\xi = x/L$. This

problem was eventually resolved by introducing the non dimensional displacement, v^* , defined as,

$$v^* = \frac{v}{L} \quad (29)$$

Its derivatives,

$$\begin{aligned} \frac{\partial v^*}{\partial v} &= \frac{1}{L} \\ \frac{\partial v}{\partial v^*} &= L \end{aligned} \quad (30)$$

are used such that,

$$\begin{aligned} v_{\xi} &= \frac{\partial v}{\partial \xi} = \frac{\partial}{\partial \xi} (Lv^*) = Lv_{\xi}^* \\ v_{\xi\xi} &= \frac{\partial}{\partial \xi} (v_{\xi}) = \frac{\partial}{\partial \xi} (Lv_{\xi}^*) = Lv_{\xi\xi}^* \end{aligned} \quad (31)$$

and in the same fashion,

$$v_{\xi\xi\xi} = Lv_{\xi\xi\xi}^* \quad (32)$$

and,

$$v_{\xi\xi\xi\xi} = Lv_{\xi\xi\xi\xi}^* \quad (33)$$

After making the substitutions into the equations of lateral and axial motion, Equations (25) and (28) respectively, the spatially non dimensional Euler equations are obtained.

a. Final Euler Equation of Lateral Motion

$$v_{\xi\xi\xi\xi}^* + \beta \left[\xi^2 \frac{L^2}{L} v_{\xi\xi}^* + 2\xi \frac{L^2}{L} v_{\xi}^* - 2\xi L v_{\xi\eta}^* - \xi \dot{L} v_{\xi}^* + L v_{\eta\eta}^* \right] = P^*(\xi, \eta) \quad (34)$$

$$0 < \xi < 1$$

$$0 < \eta$$

where,

$$\beta = \frac{\rho L^3}{EI}, \text{ and} \quad (35)$$

$$P^* = \frac{L^3}{EI} P(\xi, \eta)$$

and its boundary conditions are,

$$\begin{aligned} v^*(0, \eta) &= 0 & v_{\xi\xi}^*(1, \eta) &= 0 \\ v_{\xi}^*(0, \eta) &= 0 & v_{\xi\xi\xi}^*(1, \eta) &= 0 \end{aligned} \quad (36)$$

Again, discussion of the initial conditions will be delayed until later.

b. Final Euler Equation of Axial Motion

$$\ddot{L} + \frac{1}{2\rho L_0} \left(\frac{EI}{L^2} v_{\xi\xi}'(1,\eta) - \rho [-\dot{L} v_{\xi}'(1,\eta) + L v_{\eta}'(1,\eta)]^2 \right) = \frac{1}{2\rho L_0} F(\eta) \quad (37)$$

$$0 < \xi < 1$$

$$0 < \eta$$

and initial conditions,

$$\begin{aligned} L(0) &= L_0 \\ \dot{L}(0) &= \dot{L}_0 \end{aligned} \quad (38)$$

F. CASES

There are two general cases for which the transient behavior of the cantilever beam may be considered. Recall that the beam is free to move axially when an axial force $F(t)$ is applied resulting in an axial displacement, or when an axial displacement $L(t)$ is otherwise imposed. It was shown in the Euler equation of axial motion (Eq. 37) that the axial motion described by $L(t)$ depends on $F(t)$. However, if this axial motion is specified simply as some function of time alone then the problem is greatly simplified.

1. Case One, $L(t)$ Prescribed

If $L(t)$ is known then the problem is reduced to finding a solution to the Euler equation of lateral motion (Eq. 34) subject to its boundary and initial conditions. The problem is a linear, initial-boundary value problem.

An even further simplification occurs if the axial motion is so slow that the time derivatives of $L(t)$ are negligible. Certain linear functions of $L(t)$ can conveniently provide such a condition where the rate (or velocity) is made small, and the second time derivative (acceleration) is always zero. In this case Equation (34) reduces to,

$$v_{\xi\xi\xi\xi}^* + \frac{\rho L^4}{EI} v_{\eta\eta}^* = 0 \quad (39)$$

subject to its boundary and initial conditions and where $p^*(\xi, \eta) = 0$ for a beam with no internal loading. Note that L^4 is not a constant here, since $L(t)$ is a prescribed function of time which needs to be known.

In either of the cases (Eqs. (35) or (39)), a closed form solution to the equation(s) is not possible. The finite element method (FEM), to be presented in Chapter III, was used to obtain approximate solutions for both of these cases.

2. Case Two, $F(t)$ Prescribed

In the case where $F(t)$ is prescribed, both Equations (34) and (37), subject to their respective boundary and

initial conditions must be solved. We recall, that together these two equations form a coupled, initial-boundary value problem. Moreover, they are both now nonlinear, as they contain terms with both dependent variables, L and v and their derivatives. Therefore, it is necessary to linearize both equations.

Any number of different strategies are possible for the linearization of these equations. The strategy used here will be to treat each dependent variable as a 'primary' or 'secondary' variable in accordance with the following scheme. The assignment of 'primary' or 'secondary' status will differ depending upon which equation is to be linearized. In the linearization of the equation of lateral motion, the 'primary' variables are lateral deflection, v and its derivatives; and the 'secondary' variables are axial motion, L and its derivatives. As 'secondary' variables in the equation for lateral motion, L and its derivatives are evaluated at the previous time. On the other hand, for the equation of axial motion, L and its derivatives are considered the 'primary' variables and v and its derivatives are the 'secondary' variables. In this case v and its derivatives are evaluated at the previous time step.

The linearization of Equation (34) is quite simple because in the nonlinear product terms, the primary variables (v and its derivatives) appear linearly. Therefore, it only becomes necessary to evaluate the secondary variables in these

product terms at the previous time. For completeness the linearized equation is shown below,

$$v_{\xi\xi\xi\xi}^* + \beta \cdot \left[\xi^2 \left(\frac{\dot{L}^2}{L} \right) v_{\xi\xi}^* + 2\xi \left(\frac{\dot{L}^2}{L} \right) v_{\xi}^* - 2\xi \dot{L} \cdot v_{\xi\eta}^* - \xi \dot{L} \cdot v_{\xi}^* + L \cdot v_{\eta\eta}^* \right] = p^*(\xi, \eta).$$

$$0 < \xi < 1$$

$$0 < \eta$$

(40)

where the * subscript on a variable (or term) denotes that the variable (or term) is evaluated at the previous time and therefore is not an unknown in the equation.

The linearization of Equation (37) is not so simple because the primary variables (L and its derivatives) do not appear linearly in the nonlinear product terms.

If Equation (37) is expanded,

$$\begin{aligned} \ddot{L} + \frac{1}{2\rho L_0} \left[\frac{v_{\xi\xi}^{*2}(1, \eta)}{L^2} \right] - \frac{1}{2L_0} [\dot{L}^2 v_{\xi}^{*2}(1, \eta)] + \frac{1}{L_0} [L\dot{L} v_{\xi}^{*2}(1, \eta) \cdot v_{\eta}^*(1, \eta)] \\ - \frac{1}{2} L_0 [L^2 v_{\eta}^{*2}(1, \eta)] = \frac{1}{2\rho L_0} F(\eta) \end{aligned} \quad (41)$$

each of the bracketed [] terms are nonlinear. These terms can be linearized in a number of different ways. Since this is primarily an "L" equation, the "L" operators will be

linearized using the quasilinearization technique of Bellman & Kalaba [Ref.2]. The nonlinear terms then become,

$$\begin{aligned}
 1. \quad \frac{v_{\xi\xi}^{*2}(1, \eta)}{L^2} &\approx v_{\xi\xi}^{*2}(1, \eta) \left\langle \frac{3}{L_*^2} - \frac{2}{L_*^3} L \right\rangle \\
 \text{where, } v_{\xi\xi}^{*2}(1, \eta) &\approx \left[-\frac{6}{L_*^2} v_*(1, \eta) + \frac{4}{L_*} \theta_*(1, \eta) \right]^2 \quad (42) \\
 2. \quad L^2 v_{\xi}^{*2}(1, \eta) &\approx [\theta_*(1, \eta)]^2 (-L_*^2 + 2L_* L) \\
 3. \quad L L v_{\xi}^*(1, \eta) v_{\eta}^*(1, \eta) &\approx \theta(1, \eta) v_*(1, \eta) L_* L \\
 4. \quad L^2 v_{\eta}^{*2}(1, \eta) &\approx v_*^2(1, \eta) (-L_*^2 + 2L_* L)
 \end{aligned}$$

where L_* is the length of a finite element after the beam is discretized, θ represents slope v_{ξ} . Recalling that $\eta=t$, in these equations, the subscript η denotes partial differentiation with respect to time. Again, the * subscript on a variable (or term) denotes that the value of the variable (or term) from the previous integration is used.

Equation (37) can be rewritten in terms of the L operators and the following groups of terms,

$$\begin{aligned}
C_1 &= \frac{EI}{2\rho L_0} \cdot \frac{3}{L_*^2} \left[-\frac{6}{L_*^2} v_*(1, \eta) + \frac{4}{L_*} \theta_*(1, \eta) \right]^2 \\
C_2 &= -\frac{EI}{2\rho L_0} \cdot \frac{2}{L_*^3} \left[-\frac{6}{L_*^2} v_*(1, \eta) + \frac{4}{L_*} \theta_*(1, \eta) \right]^2 \\
C_3 &= \frac{1}{2L_0} \theta_*^2(1, \eta) L_*^2 \\
C_4 &= -\frac{2}{2L_0} \theta_*^2(1, \eta) L_* \\
C_5 &= \frac{1}{L_0} \theta_*(1, \eta) v_*(1, \eta) L_* \\
C_6 &= \frac{1}{2L_0} v_*^2(1, \eta) L_*^2 \\
C_7 &= -\frac{2}{2L_0} v_*^2(1, \eta) L_* \\
C_8 &= \frac{1}{2\rho L_0}
\end{aligned} \tag{43}$$

Using Equations (43), Equation (37) becomes,

$$\ddot{L} + C_1 + C_2 L + C_3 + C_4 \dot{L} + C_5 L + C_6 + C_7 L = C_8 F(\eta) \tag{44}$$

Equation (40), its boundary and initial conditions, and Equation (44) with its initial conditions, now form a coupled, linear initial-boundary value problem. A closed form solution of these equations is not possible. The finite element method (FEM), to be presented in Chapter III, could be used to obtain approximate solutions to these equations.

III. SOLUTION METHOD

A. FINITE ELEMENT METHOD DEVELOPMENT

Considering the $L(t)$ specified case first, the task is to solve Equation (34) together with its boundary conditions given by Equation (36), and its initial conditions as determined by the problem being investigated. Definition of the initial conditions will require further discussion which will be conducted later in this development.

Equation (34) is a linear partial differential equation in one unknown, $v'(\xi, t)$ when $L(\tau)$ is specified. Recalling that $\eta = t$, here t will replace η . An approximate numerical solution of this equation together with its initial and boundary conditions can be obtained by a Galerkin finite element formulation.

1. Construction of the Beam Element

The fourth order system of Equation (34) requires C^1 continuity (continuity of function and slope). In order to obtain C^1 continuity, an element with deflection v' , and slope θ' , (θ' will represent v'_ξ in the development that follows, as degrees of freedom (DOF) at each end point is required. This means each element must have a minimum of four DOF, which requires a cubic polynomial. These interpolation polynomials

are the set of cubic spline shape functions listed below and detailed in Appendix A.

$$\begin{aligned}
 q_1 &= 1 - \frac{3}{l_\bullet^2} \alpha^2 + \frac{2}{l_\bullet^3} \alpha^3 \\
 q_2 &= \alpha - \frac{2}{l_\bullet} \alpha^2 + \frac{1}{l_\bullet^2} \alpha^3 \\
 q_3 &= \frac{3}{l_\bullet^2} \alpha^2 - \frac{2}{l_\bullet^3} \alpha^3 \\
 q_4 &= -\frac{1}{l_\bullet} \alpha^2 + \frac{1}{l_\bullet^2} \alpha^3
 \end{aligned} \tag{45}$$

Figure (A.1) shows that shape functions q_1 and q_3 , are associated with the displacement DOF (v_1^* , v_2^* where subscripts 1 and 2 represent node points 1 and 2) at the element end points; and the even numbered shape function q_2 and q_4 , are associated with the slope DOF (θ_1^* , θ_2^*) at the same locations.

2. Global FEM Formulation

In terms of global shape functions Q_i , the FEM approximation v^* to \tilde{v}^* is given by,

$$v^* \approx \tilde{v}^* = \mathbf{Q}^T \boldsymbol{\delta} = \sum_{i=1}^{\bar{N}} Q_i \delta_i \tag{46}$$

where N is the number of elements, $\bar{N} = 2N + 2$ is the number of

global DOF, and δ_i are the global degrees of freedom. The global degrees of freedom, δ_i are defined as follows,

$$\delta^T = \langle \delta_1 \delta_2 : \delta_3 \delta_4 : \delta_5 \delta_6 : \dots : \delta_{\bar{N}-1} \delta_{\bar{N}} \rangle \quad (47)$$

where subscripts 1,2,3,...(\bar{N} -1) are DOF identifiers. In terms of displacements and slopes, we have,

$$\delta^T = \langle v_1 \theta_1 : v_2 \theta_2 : v_3 \theta_3 : \dots : v_{N+1} \theta_{N+1} \rangle^* \quad (48)$$

where the subscripts 1,2,3,...($N+1$) refer to the Global Nodal Points (GNP) and, $\langle \rangle^*$ indicates the non dimensional forms of v and θ , that is v^* and θ^* .

The relationship between the global degrees of freedom δ_i and, \tilde{v}^* and $\tilde{\theta}^*$; is such that for odd i (1,3,5,... \bar{N} -1); $\delta_i = \tilde{v}^*$ at GNP [($i+1$)/2]. (i.e., $\delta_1 = \tilde{v}^*(\text{GNP } 1)$, $\delta_3 = \tilde{v}^*(\text{GNP } 2)$, ...) For even i (2,4,6,... \bar{N}); $\delta_i = \tilde{\theta}^*$ at GNP [$i/2$]. (i.e., $\delta_2 = \tilde{\theta}^*(\text{GNP } 1)$, $\delta_4 = \tilde{\theta}^*(\text{GNP } 2)$, ...)

Each i^{th} GNP has two global shape functions, and hence two DOF. An odd numbered shape function Q_i , gives displacement \tilde{v}^* at $\text{GNP}\{(i+1)/2\} = v_{((i+1)/2)}^* = \delta_i$, and an even

numbered shape function Q_i , gives slope θ_i at

$$GNP\{i/2\} = \theta_{(i/2)} = \delta_i.$$

3. Galerkin FEM Formulation

In accordance with the Galerkin Finite Element Method (FEM), we form the approximate solution of v ,

$$v^*(\xi, t) \approx \tilde{v}^*(\xi, t) = \mathbf{Q}^T(\xi) \delta(t) \quad (49)$$

Using the above approximation, the residual function for the Euler equation of lateral motion (Eq. 34) is,

$$R(\xi, t) = \mathcal{L}\{\tilde{v}^*\} - p^* \quad (50)$$

or,

$$R(\xi, t) = (\tilde{v}^*)_{\xi\xi\xi\xi} + \beta \left[\xi^2 \frac{\dot{L}^2}{L} (\tilde{v}^*)_{\xi\xi} + 2\xi \frac{\dot{L}^2}{L} (\tilde{v}^*)_{\xi} - 2\xi \dot{L} (\tilde{v}^*)_{\xi} - \xi \dot{L} (\tilde{v}^*)_{\xi} + L\ddot{\tilde{v}}^* \right] - p^* \quad (51)$$

After the final substitution, the residual is,

$$R(\xi, t) = (Q^T)_{\xi\xi\xi\xi} \delta + \beta \left[\xi^2 \frac{\dot{L}^2}{L} (Q^T)_{\xi\xi} \delta + 2\xi \frac{\dot{L}^2}{L} (Q^T)_{\xi} \delta - 2\xi \dot{L} (Q^T)_{\xi} \delta - \xi \dot{L} (Q^T)_{\xi} \delta + L Q^T \delta \right] - P^* \quad (52)$$

The Galerkin finite element equation is obtained by requiring that the residual function be orthogonal to each of the basis functions. That is,

$$\int_0^1 Q R d\xi = 0 \quad (53)$$

Substitution of Equation (51) into Equation (52) gives,

$$\begin{aligned} & \int_0^1 Q (Q^T)_{\xi\xi\xi\xi} d\xi \delta + \beta \frac{\dot{L}^2}{L} \int_0^1 \xi^2 Q (Q^T)_{\xi\xi} d\xi \delta + \\ & 2\beta \frac{\dot{L}^2}{L} \int_0^1 \xi Q (Q^T)_{\xi} d\xi \delta - 2\beta \dot{L} \int_0^1 \xi Q (Q^T)_{\xi} d\xi \delta - \\ & \beta \dot{L} \int_0^1 \xi Q (Q^T)_{\xi} d\xi \delta + \beta L \int_0^1 Q (Q^T) d\xi \delta = \int_0^1 Q P^* d\xi \end{aligned} \quad (54)$$

After performing two integrations by parts on the first term
(See Appendix D), Equation (53) becomes,

$$\begin{aligned}
\mathbf{B.T.} &+ \int_0^1 Q_{\xi\xi} (Q^T)_{\xi\xi} d\xi \delta + \beta \frac{L^2}{L} \int_0^1 \xi^2 Q (Q^T)_{\xi\xi} d\xi \delta + \\
&2\beta \frac{L^2}{L} \int_0^1 \xi Q (Q^T)_{\xi} d\xi \delta - 2\beta L \int_0^1 \xi Q (Q^T)_{\xi} d\xi \delta - \\
&\beta L \int_0^1 \xi Q (Q^T)_{\xi} d\xi \delta + \beta L \int_0^1 Q (Q^T) d\xi \delta = \int_0^1 Q P^* d\xi
\end{aligned} \tag{55}$$

where $\mathbf{B.T.}$ is the vector of boundary terms resulting from the
two integrations by parts,

$$\mathbf{B.T.} = Q(\bar{V}^*)_{\xi\xi\xi} \Big|_0^1 - Q_{\xi}(\bar{V}^*)_{\xi\xi} \Big|_0^1 \tag{56}$$

The kronecker delta property of the shape functions Q_i ,
results in the reduction of the boundary term vector to,

$$\mathbf{B.T.} = \begin{Bmatrix} -(\bar{V}^*)_{\xi\xi\xi}(0) \\ (\bar{V}^*)_{\xi\xi}(0) \\ 0 \\ 0 \\ \vdots \\ 0 \\ 0 \\ (\bar{V}^*)_{\xi\xi\xi}(1) \\ -(\bar{V}^*)_{\xi\xi}(1) \end{Bmatrix} \tag{57}$$

The non zero terms in the B.T. vector represent the non dimensionalized loads and moments applied at the boundaries. If there is no applied load (or moment) at the boundary, then B.T. is simply the zero vector.

A discussion of the second term of Equation (54) follows. The integration by parts performed on the first term of Equation (54) results in a self adjoint (symmetric) operator, a condition which is generally desired since it reduces storage requirements during computer processing. Integration by parts on the second term,

$$\int_0^1 \xi^2 Q(Q^T)_{\xi\xi} d\xi \delta \quad (58)$$

results in a B.T. on $\tilde{\theta}^*$ evaluated at $\xi = 1$. Since the value of $\tilde{\theta}^*(1)$ is unknown, an integration by parts was not performed on the $v_{\xi\xi}$.

Letting,

$$\begin{aligned}
 \mathbf{A} &= \int_0^1 \mathbf{Q}_{\xi\xi} (\mathbf{Q}^T)_{\xi\xi} d\xi \\
 \mathbf{B} &= \int_0^1 \xi^2 \mathbf{Q} (\mathbf{Q}^T)_{\xi\xi} d\xi \\
 \mathbf{C} &= \int_0^1 \xi \mathbf{Q} (\mathbf{Q}^T)_{\xi} d\xi \\
 \mathbf{D} &= \int_0^1 \mathbf{Q} (\mathbf{Q}^T)_{\xi} d\xi \\
 \mathbf{F} &= \int_0^1 \mathbf{Q} \mathbf{P}^* d\xi - \mathbf{B.T.}
 \end{aligned} \tag{59}$$

the final Galerkin Equation is,

$$\begin{aligned}
 \mathbf{A} \delta + \beta \frac{\bar{L}^2}{L} \mathbf{B} \delta + 2\beta \frac{\bar{L}^2}{L} \mathbf{C} \delta - \\
 2\beta \bar{L} \mathbf{C} \dot{\delta} - \beta \bar{L} \mathbf{C} \delta + \beta L \mathbf{D} \dot{\delta} = \mathbf{F}
 \end{aligned} \tag{60}$$

The details of the construction and form of the \mathbf{A} , \mathbf{B} , \mathbf{C} , and \mathbf{D} matrices are contained in Appendix B.

4. Integration of the Galerkin Equation

a. Reduction of the Second Order System

Equation (59) is a system of second order ordinary differential equation in time. For numerical integration purposes, it is desirable to reduce this second order system to a first order system in time.

For compactness, let,

$$\begin{aligned} K &= -\frac{1}{L} \left[\frac{1}{\beta} A + \frac{\dot{L}^2}{L} B + \left(\frac{2\dot{L}^2}{L} - \ddot{L} \right) C \right] \\ M &= \frac{2\dot{L}}{L} C \\ P &= \frac{1}{\beta L} F \end{aligned} \tag{61}$$

Then, Equation (59) becomes,

$$D \ddot{\delta} = M \dot{\delta} + K \delta + P \tag{62}$$

Letting $\omega = \dot{\delta}$, it follows that,

$$\dot{\omega} = \ddot{\delta} \tag{63}$$

and Equation (59) now becomes the first order system of equations,

$$\begin{aligned} \dot{\delta} &= \omega \\ D\dot{\omega} &= M\dot{\delta} + K\delta + P \end{aligned} \tag{64}$$

In explicit matrix form, Equations (62) and (63) may be written,

$$\begin{bmatrix} \mathbf{I} & : & \mathbf{0} \\ \dots & & \dots \\ \mathbf{0} & : & \mathbf{D} \end{bmatrix} \begin{Bmatrix} \dot{\delta} \\ \dots \\ \dot{\omega} \end{Bmatrix} = \begin{bmatrix} \mathbf{0} & : & \mathbf{I} \\ \dots & & \dots \\ \mathbf{K} & : & \mathbf{M} \end{bmatrix} \begin{Bmatrix} \delta \\ \dots \\ \omega \end{Bmatrix} + \begin{Bmatrix} \mathbf{0} \\ \dots \\ \mathbf{P} \end{Bmatrix} \quad (65)$$

Letting,

$$\mathbf{G} = \begin{bmatrix} \mathbf{I} & : & \mathbf{0} \\ \dots & & \dots \\ \mathbf{0} & : & \mathbf{D} \end{bmatrix}, \quad \dot{\lambda} = \begin{Bmatrix} \dot{\delta} \\ \dots \\ \dot{\omega} \end{Bmatrix}, \quad \mathbf{H} = \begin{bmatrix} \mathbf{0} & : & \mathbf{I} \\ \dots & & \dots \\ \mathbf{K} & : & \mathbf{M} \end{bmatrix}, \quad \lambda = \begin{Bmatrix} \delta \\ \dots \\ \omega \end{Bmatrix} \text{ and, } \Omega = \begin{Bmatrix} \mathbf{0} \\ \dots \\ \mathbf{P} \end{Bmatrix} \quad (66)$$

the second order system of Equation (59) is reduced to the following first order system in time.

$$\mathbf{G} \dot{\lambda} = \mathbf{H} \lambda + \Omega \quad (67)$$

Vector Ω , becomes the zero vector if vector \mathbf{P} is a zero vector. Referring to Equations (59) and (60) we see that \mathbf{P} is actually defined by vector \mathbf{F} which is defined further by the boundary term vector **B.T.**, and the vector describing the contribution of an internally applied load, p^* . If **B.T.** is the zero vector (no applied moment or load at the boundaries)

and there is no internally applied load, then \mathbf{P} and $\mathbf{\Omega}$ are zero vectors. Evaluation of the B.T. vector has also resulted in satisfying the natural boundary conditions imposed on Equation (34). Equation (66) now becomes,

$$\mathbf{G} \dot{\boldsymbol{\lambda}} = \mathbf{H} \boldsymbol{\lambda} \quad (68)$$

b. Boundary and Initial Conditions

Prior to integrating the system described in Equation (67), the boundary and initial conditions on Equation (34) must be imposed. The boundary conditions at the free end ($\xi=1$), were imposed through the boundary term vector as previously described. The strategy used to impose the essential boundary conditions at the "fixed end" ($\xi=0$), is one in which the deflection and slope at the "fixed end" are set to zero when the $\boldsymbol{\lambda}$ vector is initialized, and the \mathbf{G} and \mathbf{H} matrices are altered such that the deflection and slope at $\xi = 0$, remain constant with time. If the first and second time derivatives of deflection and slope at $\xi = 0$ are constant and equal to zero, then the desired conditions of zero deflection and slope at $\xi = 0$ are obtained providing that the initial conditions on deflection ($v(0,0) = 0$), and slope ($\theta(0,0) = 0$), are satisfied.

Initial conditions are imposed through the initialization of the $\boldsymbol{\lambda}$ vector in accordance with the problem being investigated. Referring back to the global FEM

formulation, we recall that each nodal point has two DOF. To satisfy the two DOF, deflection (and its velocity), as well as slope (and its velocity), must be initially defined at each node. The initial conditions must also satisfy the essential boundary conditions at $\xi = 0$. The initial conditions are more clearly understood if the λ vector is given in greater detail,

$$\lambda_0 = \left\{ \begin{array}{c} v_1 \\ \theta_1 \\ \vdots \\ v_{\bar{N}-1} \\ v_{\bar{N}} \\ \dots \\ \dot{v}_1 \\ \dot{\theta}_1 \\ \vdots \\ \dot{v}_{\bar{N}-1} \\ \dot{\theta}_{\bar{N}} \end{array} \right\}^* \quad (69)$$

where the * subscript indicates the terms are the non dimensional variables (and their derivatives) and therefore, are functions of ξ , not x .

The matrices and vectors of Equation (67), modified for the boundary and initial conditions follow,

$$G = \begin{bmatrix} & & \vdots & & \\ & & \vdots & & \\ & I & \vdots & 0 & \\ & & \vdots & & \\ & & \vdots & & \\ & & \vdots & & \\ & & \vdots & & \\ \dots & \dots & \vdots & \dots & \dots \\ & & \vdots & 1 & 0 & 0 & \dots & 0 & 0 & 0 \\ & & \vdots & 0 & 1 & 0 & \dots & 0 & 0 & 0 \\ & 0 & \vdots & & & D & & & & \\ & & \vdots & & & & & & & \\ & & \vdots & & & & & & & \\ & & \vdots & & & & & & & \end{bmatrix} \quad (70)$$

where only the first two rows of D are altered as shown and,

(71)

as shown and,

(72)

and,

$$\lambda = \begin{Bmatrix} \delta \\ \dots \\ \omega \end{Bmatrix} = \begin{Bmatrix} v_1 \\ \theta_1 \\ \vdots \\ v_{\bar{N}-1} \\ v_{\bar{N}} \\ \dots \\ \dot{v}_1 \\ \dot{\theta}_1 \\ \vdots \\ \dot{v}_{\bar{N}-1} \\ \dot{\theta}_{\bar{N}} \end{Bmatrix}_{t_1} \quad (73)$$

B. FEM VERIFICATION

The static cantilever beam provides a problem for which a known solution is available for comparison and verification of the FEM development and Fortran code.

For the static cantilever beam, the Euler equation of lateral motion (Eq. 1) is reduced to,

$$EIV_{xxxx}(x) = p(x) \quad 0 < x < L \quad (74)$$

with the boundary conditions,

$$\begin{aligned} v(0) &= 0 & EIV_{xx}(L) &= M \text{ (moment)} \\ v_x(0) &= 0 & EIV_{xxx}(L) &= P \text{ (load)} \end{aligned} \quad (75)$$

Referring to the Euler equation of lateral motion (Eq. 25), and considering that for the static cantilever beam,

$$\begin{aligned} \dot{L} &= \ddot{L} = 0 \\ \ddot{\delta} &= 0 \end{aligned} \quad (76)$$

Equation (73) transformed to the non dimensional coordinate ξ becomes,

$$v_{\xi\xi\xi\xi} = \frac{L^4}{EI} P(\xi) \quad 0 < \xi < 1 \quad (77)$$

with the boundary conditions,

$$\begin{aligned} v(0) &= 0 & \frac{EI}{L^2} v_{\xi\xi}(1) &= M \\ v_{\xi}(0) &= 0 & \frac{EI}{L^3} v_{\xi\xi\xi}(1) &= P \end{aligned} \quad (78)$$

Referring to Equation (34), the final spatially non dimensional static beam equation, where the lateral deflection

has also been non dimensionalized, becomes,

$$v_{\xi\xi\xi\xi}^*(\xi) = \frac{L^3}{EI} P(\xi) \quad 0 < \xi < 1 \quad (79)$$

with the boundary conditions,

$$\begin{aligned} v^*(0) &= 0 & \frac{EI}{L} v_{\xi\xi}^*(1) &= M \\ v_{\xi}^*(0) &= 0 & \frac{EI}{L^2} v_{\xi\xi\xi}^*(1) &= P \end{aligned} \quad (80)$$

The Galerkin FEM formulation for Equation (78) and its boundary conditions is obtained from Equation (59). Again, recalling that,

$$\begin{aligned} \dot{L} &= \dot{L} = 0 \\ \ddot{\delta} &= 0 \end{aligned} \quad (81)$$

Equation (59) becomes,

$$A \delta = F \quad (82)$$

where,

$$F = \int_0^1 Q P^* d\xi - B.T. \quad (83)$$

and, if there is no excitation internal to the system other than at the boundaries ($p^* = 0$) then,

$$F = 0 - B.T. \quad (84)$$

The boundary conditions given in Equations (79), must be imposed prior to solving the system of Equation (81). To do this the boundary term vector **B.T.**, resulting from the integration by parts on the $\tilde{v}_{\xi\xi\xi}^*$ operator and shown in Equation (56),

$$B.T. = \left\{ \begin{array}{c} -\tilde{v}_{\xi\xi\xi}^*(0) \\ \tilde{v}_{\xi\xi}^*(0) \\ 0 \\ 0 \\ \vdots \\ 0 \\ 0 \\ \tilde{v}_{\xi\xi\xi}^*(1) \\ -\tilde{v}_{\xi\xi}^*(1) \end{array} \right\} \quad (56)$$

is evaluated using the boundary conditions at the free end of the beam ($\xi = 1$).

Rearrangement of terms in Equations (79) gives,

$$\begin{aligned} v_{\xi\xi}^*(1) &= \frac{ML}{EI} \\ v_{\xi\xi\xi}^*(1) &= \frac{PL^2}{EI} \end{aligned} \quad (86)$$

The B.T. vector can be rewritten as,

$$\mathbf{B.T.} = \begin{Bmatrix} -\tilde{v}_{\xi\xi\xi}^*(0) \\ \tilde{v}_{\xi\xi}^*(0) \\ 0 \\ 0 \\ \vdots \\ 0 \\ 0 \\ \frac{PL^2}{EI} \\ -\frac{ML}{EI} \end{Bmatrix} \quad (87)$$

Next the boundary conditions at the fixed end ($\xi = 0$) are imposed. Recalling that $\delta_1 \approx v_1^* = v^*(0)$ and $\delta_2 \approx \theta_1^* = \theta^*(0)$, the boundary conditions at the fixed end are imposed by altering the first two rows of both the **A** matrix, and the B.T. vector to force δ_1 and δ_2 to zero.

The final system can be written as,

$$\begin{bmatrix} 1 & 0 & 0 & \dots & 0 & 0 & 0 \\ 0 & 1 & 0 & \dots & 0 & 0 & 0 \\ A_{31} & & & \dots & & & A_{3N} \\ \vdots & & & & & & \vdots \\ A_{N1} & & & \dots & & & A_{NN} \end{bmatrix} \begin{Bmatrix} \delta_1 \\ \delta_2 \\ \vdots \\ \delta_{\bar{N}-1} \\ \delta_{\bar{N}} \end{Bmatrix} = \begin{Bmatrix} 0 \\ 0 \\ \vdots \\ -\frac{PL^2}{EI} \\ \frac{ML}{EI} \end{Bmatrix} \quad (88)$$

where \bar{N} is the number of degrees of freedom.

The solution to this system is,

$$\delta = \begin{Bmatrix} v_1^* \\ \theta_1^* \\ \vdots \\ v_N^* \\ \theta_N^* \end{Bmatrix} \quad (89)$$

If $\frac{PL^2}{EI}$ (or $\frac{ML}{EI}$) is set at unity, then to obtain the δ for actual values of $\frac{PL^2}{EI}$ (or $\frac{ML}{EI}$), the δ vector is multiplied by $\frac{PL^2}{EI}$ (or $\frac{ML}{EI}$).

The exact solutions for the deflection and slope at the free end of a cantilever beam subject to a concentrated load (or moment) are obtained from the following expressions,

$$\begin{aligned} v(L) &= \frac{PL^3}{3EI} & \theta(L) &= \frac{PL^2}{2EI} \\ v(L) &= \frac{ML^2}{2EI} & \theta(L) &= \frac{ML}{EI} \end{aligned} \quad (90)$$

where P (or M) is the load (or moment) applied at the free end.

The δ vector is the vector of non dimensional deflections, and slopes. The dimensional vector is obtained by multiplying the non dimensional displacements (δ_i for odd i) by L in accordance with $v = Lv^*$. Since slope is a non dimensional quantity to begin with, the θ^* 's (δ_i for even i) are equal to the θ 's.

The Fortran code used for this verification and comparison is located in Appendix C. Results of the verification, also in Appendix C, confirm the FEM development.

C. THE $F(t)$ PRESCRIBED SOLUTION METHOD

The final and most complex case posed in Chapter II was the case where the axial force, $F(T)$ is prescribed. In this case an equation for axial motion, in addition to the Euler equation of lateral motion, was required. That equation was the Euler equation of axial motion. Together these two equations form a nonlinear, coupled, initial-boundary value problem. After the linearization of these equations, the linear, coupled, initial-boundary value problem consisted of the following equations,

$$v_{\xi\xi\xi\xi}^* + \beta \cdot \left[\xi^2 \left(\frac{\dot{L}^2}{L} \right) v_{\xi\xi}^* + 2\xi \left(\frac{\dot{L}^2}{L} \right) v_{\xi}^* - 2\xi \dot{L} \cdot v_{\xi\eta}^* - \xi \dot{L} \cdot v_{\xi}^* + L \cdot v_{\eta\eta}^* \right] = p^*(\xi, \eta) = 0 \quad (91)$$

$$\ddot{L} + C_1 + C_2 L + C_3 + C_4 \dot{L} + C_5 L + C_6 + C_7 \dot{L} = C_8 F(\eta) \quad (92)$$

where $p^* = 0$ for the no internal excitation case, and C_i are defined in Equations (43).

By defining new terms, J_1 which require updating during the time integration process,

$$\begin{aligned} J_1(t) &= C_2 + C_5 + C_7 \\ J_2(t) &= C_4 \\ J_3(T) &= C_1 + C_3 + C_6 \end{aligned} \tag{93}$$

Equation (45) becomes,

$$\ddot{L} + J_1 L + J_2 \dot{L} = C_8 F(t) - J_3 \tag{94}$$

Equation (93) is a second order differential equation in time. Letting,

$$\begin{aligned} \mathcal{L} &= \dot{L} \\ \dot{\mathcal{L}} &= \ddot{L} \end{aligned} \tag{95}$$

and using substitution, the following system of two first order differential equations is obtain;

$$\begin{aligned} \mathcal{L} &= \dot{L} \\ \dot{\mathcal{L}} + J_1 L + J_2 \mathcal{L} &= C_8 F(t) - J_3 \end{aligned} \tag{96}$$

Since $L(t)$ and its derivatives do not depend on a spatial variable, Equations (95) do not require a FEM formulation and are directly added to the system of equations for lateral

motion. The matrix equations for lateral motion will be similar in structure to the system of Equation (64). However, the 'secondary' variables (or terms) introduced in the linearization of the equation, are assigned their values from the previous integration. Therefore, the sub matrices D , K , and M which contain these variables (or terms), appear with the * subscript. Ω is the zero vector because there is no internal excitation, and the natural boundary conditions used to evaluate the B.T. vector are equal to zero (moment=load=0). The matrix system of equations which is obtained after adding Equations (95) to the system in Equation (96) is shown here,

$$\begin{bmatrix} I & : & 0 \\ \dots & & \dots \\ 0 & : & D_* \end{bmatrix} \begin{Bmatrix} \dot{\delta} \\ \dots \\ \dot{\omega} \end{Bmatrix} = \begin{bmatrix} 0 & : & I \\ \dots & & \dots \\ K_* & : & M_* \end{bmatrix} \begin{Bmatrix} \delta \\ \dots \\ \omega \end{Bmatrix} + \begin{Bmatrix} 0 \\ \dots \\ 0 \end{Bmatrix} \quad (97)$$

The final system for the $F(t)$ prescribed case is,

$$\begin{bmatrix} & & & & 0 & 0 \\ & I & & 0 & & \\ & & & & & \\ \dots & \dots & \dots & \dots & \dots & \dots \\ & 0 & & D_s & & \\ & & & & 0 & 0 \\ \dots & \dots & \dots & \dots & \dots & \dots \\ 0 & & \leftrightarrow & 0 & 1 & 0 \\ \dots & \dots & \dots & \dots & \dots & \dots \\ 0 & & \leftrightarrow & 0 & 0 & 1 \end{bmatrix} \begin{Bmatrix} \delta \\ \dots \\ \omega \\ \dots \\ L \\ \dots \\ \dot{g} \end{Bmatrix} =$$

$$\begin{bmatrix} & & & & 0 & 0 \\ & 0 & & I & & \\ & & & & & \\ \dots & \dots & \dots & \dots & \dots & \dots \\ & K_s & & M_s & & \\ & & & & 0 & 0 \\ \dots & \dots & \dots & \dots & \dots & \dots \\ 0 & & \leftrightarrow & 0 & 0 & 1 \\ \dots & \dots & \dots & \dots & \dots & \dots \\ 0 & & \leftrightarrow & 0 & -J_1 & -J_2 \end{bmatrix} \begin{Bmatrix} \delta \\ \dots \\ \omega \\ \dots \\ L \\ \dots \\ \dot{g} \end{Bmatrix} + \begin{Bmatrix} 0 \\ \dots \\ 0 \\ \dots \\ 0 \\ \dots \\ C_s F - J_3 \end{Bmatrix} \quad (99)$$

The boundary and initial conditions for the equation of lateral motion, and the initial conditions for the equation of

axial motion, are imposed using the strategy applied in the $L(t)$ specified case, and described in Section A of this Chapter.

IV. CASE STUDY REPORT AND CONCLUSIONS

A. GENERAL DISCUSSION

After verification of the finite element code the investigation of the transient problem began. The primary emphasis of the studies that follow is on obtaining solutions to problems, and not on investigation of numerical considerations. However, when appropriate the researcher's thoughts on such considerations will be presented.

The case studies reported are investigations of the $L(t)$ prescribed condition. For reference, the system developed in Chapter III for the $L(t)$ prescribed case is repeated here,

$$\begin{bmatrix} I & : & 0 \\ \dots & & \dots \\ 0 & : & D \end{bmatrix} \begin{Bmatrix} \dot{\delta} \\ \dots \\ \dot{\omega} \end{Bmatrix} = \begin{bmatrix} 0 & : & I \\ \dots & & \dots \\ K & : & M \end{bmatrix} \begin{Bmatrix} \delta \\ \dots \\ \omega \end{Bmatrix} \quad (100)$$

or,

$$G\dot{\lambda} = H\lambda \quad (101)$$

The above system does not reflect the alterations made to impose the boundary conditions on load and moment at the free end as the case studies addressed only the case of homogeneous

boundary conditions ($P=M=0$), with no internal excitation ($p^*=0$). Thus the P vector is the zero vector, and does not appear in the system above.

The transient problem introduces the requirement for a numerical integration method. To perform the integration on the system above, the IMSL, Inc. integration subroutine, DIVPAG was chosen. DIVPAG is a double precision first-order, initial-value, ordinary differential equation solver.

Two classes of implicit linear multi step methods are available. The first is the Adams's method and the second is the backward differentiation formula (up to fifth order), also called Gear's stiff method. An accepted measure of stiffness is the ratio of the maximum and minimum eigenvalues (λ_{\max} , λ_{\min}) of a system. A problem is considered stiff for very large $\lambda_{\max}/\lambda_{\min}$ ratios. The vibrating cantilever beam equation of motion results in a stiff system, and therefore, Gear's stiff method is used.

1. Time Step Convergence

The integration routine uses an internally determined time step such that a measure of global error does not exceed a user specified tolerance. This feature of DIVPAG provides error control to the user of the integration routine. However, a recognized short coming of this integration package as applied to this problem, is the inability to update the G matrix on the left hand side of Equation (100) at each of the

subroutine determined time steps. That is, as a result of the call structure of the subroutine, an update of the finite element matrix G for a change in $L(t)$ and its derivatives, is only possible outside of the subroutine. For this reason DIVPAG is placed in a Do Loop and the G matrix is updated at each entry to DIVPAG. Although the H matrix could be evaluated inside DIVPAG via a FNC subroutine argument of DIVPAG, in this investigation it was not. It was updated at the same time the G matrix was, that is, at each entry to DIVPAG. The accuracy of the numerical solution depends upon the frequency of updating of the G and H matrices. Entries to DIVPAG were at .025 second intervals for all case studies with the exception of the final case study for which entries were made at .01 second intervals. A rapidly changing $L(t)$ requires more updating of the matrices than would a slowly changing $L(t)$. In effect, a solution ultimately should be checked for "time grid" independence.

2. Spatial Grid Convergence

Convergence of the solution for the spatial grid is yet another consideration. The solution is a function of the number of elements (i.e., NDOF). For linear problems, it can be shown that in the limit, as the number of DOF approaches

infinity, the approximate solution of \tilde{v} approaches the exact solution v , that is,

$$\lim_{NDOF \rightarrow \infty} \tilde{v} \rightarrow v \quad (102)$$

However, for a nonlinear problem there is no guarantee, but a likelihood that the approximate solution converges to the exact solution in the limit as the number DOF approaches infinity. A preliminary study conducted during the first case study showed that negligible differences existed between the eight and sixteen element solutions for that particular problem. This was the basis for the use of an eight element solution for all subsequent problems. However, it is recognized that the FEM model changes with length (or time). Since the number of elements (NEL) is constant with time, convergence for a given NEL may change with time as well. Furthermore, the effects of material properties, geometric dimensions, and functions of $L(t)$ (and its derivatives), may also influence the NEL required for a spatial, grid independent solution.

3. Computational Effort

Related to the stiff character of the problem, is the very large amount of computational effort (CPU time) required to obtain solutions. A study of CPU requirements was not conducted. However, integration of a problem over a real time

five second period took as long as a week. Typically, DIVPAG performed its integration over $2 \cdot 10^{-6}$ second steps. Thus, every .1 second increment in time required approximately 500,000 integration steps. Processing was conducted using the Naval Postgraduate School IBM 3033 main frame time share system during weekday non peak hours (1800-0900), and weekends. During these periods, it is estimated that approximately 20 percent of time share CPU was allocated to the processing of this job. A restart capability was coded to assist in processing during non peak hours only.

4. The Case Study Beam

The case studies that follow are conducted using material properties similar to those of plexiglass. The modulus of elasticity (E) is equal to 100,000 psi. The initial length of the beam, L_0 is 10.0 inches for all case studies. Two moments of inertia of the beam cross-section (indication of beam rigidity, which effects the stiffness of the problem) are obtained from the cross-sectional dimensions shown in Figure (4.1). In recognition of the stiff nature of the problem, and in interest of solving a realistic problem in the minimum amount of time possible, our desire was to select a material with the smallest value of frequency, which is proportional to,

$$\sqrt{\frac{EI}{\rho L^4}} \quad (103)$$

Thus, for a beam of given geometry (I/L^4), plexiglass was selected as a realistic material with the smallest E/ρ ratio.

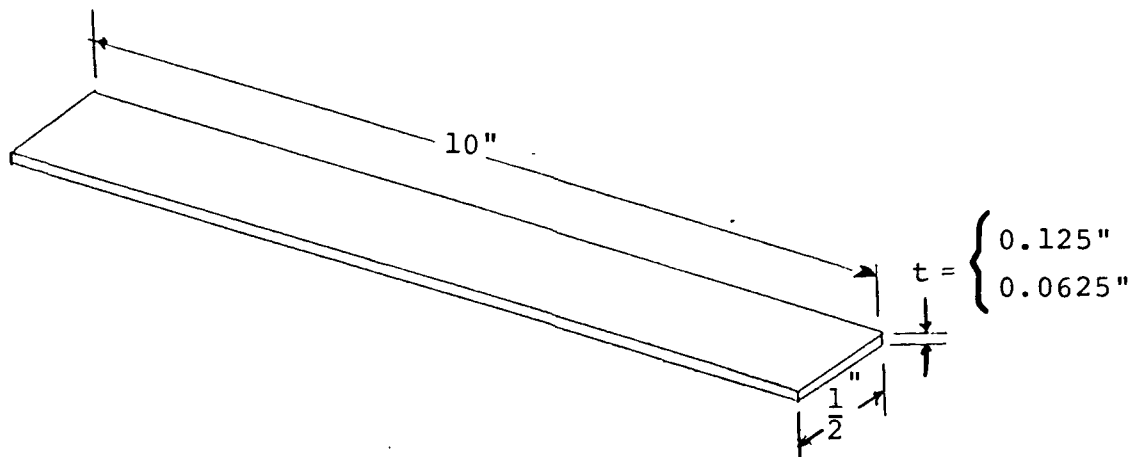


Figure 4.1 Beam Geometry

B. FIRST CASE STUDY, NEGLIGIBLE DERIVATIVES OF $L(t)$

The strategy used in the case studies is to progress from the less to the more 'difficult' cases. What is intended by 'difficult', is that fewer differential, and hence, finite element operators are involved in the Fortran coding for the less difficult case. The general program development logic is the same for all the transient case studies, however; it is generally good practice to limit the size of the code until the logic is tested and functioning as expected. By eliminating the derivatives of $L(t)$, only the **A** part of the **K** matrix (See Equation (105)) and the **D** matrix of Equation (99) need to be evaluated.

If the derivatives of the specified function of $L(t)$ are zero or negligible, the equation of lateral motion is,

$$v_{\xi\xi\xi\xi}^* + \frac{\rho L^4}{EI} v_{\eta\eta}^* = 0 \quad (104)$$

subject to boundary and initial conditions.

For this case, the matrix system of Equation (99) becomes,

$$\begin{bmatrix} \mathbf{I} & \mathbf{0} \\ \dots & \dots \\ \mathbf{0} & \mathbf{D} \end{bmatrix} \begin{Bmatrix} \dot{\delta} \\ \dots \\ \dot{\omega} \end{Bmatrix} = \begin{bmatrix} \mathbf{0} & \mathbf{I} \\ \dots & \dots \\ \mathbf{K} & \mathbf{0} \end{bmatrix} \begin{Bmatrix} \delta \\ \dots \\ \omega \end{Bmatrix} \quad (105)$$

where the \mathbf{K} sub matrix,

$$\mathbf{K} = -\frac{1}{L} \left[\frac{1}{\beta} \mathbf{A} + \frac{L^2}{L} \mathbf{B} + \left(\frac{2L^2}{L} - \dot{L} \right) \mathbf{C} \right] \quad (106)$$

is reduced to,

$$\mathbf{K} = -\frac{1}{L\beta} \mathbf{A} \quad (107)$$

This case was examined for the plexiglass beam with the larger cross sectional dimensions. The material and geometric properties used are ρ (mass/unit length) = $6.988\text{E-}6$ lbf·S²/in² (slugs/in) and, moment of inertia $I = 81.38\text{E-}6$ in⁴.

The homogenous boundary conditions are imposed as described in Chapter III. The initial conditions (λ vector) are imposed by an initial parabolic deformation (Fig. 4.2) of the beam. The λ vector is initialized for all DOF according to the following displacements (and slopes),

$$\begin{aligned} v^*(\xi, 0) &= .1\xi^2 \\ v_\xi^*(\xi, 0) &= .2\xi \end{aligned} \quad (108)$$

and velocities of displacements and slopes,

$$\begin{aligned} \dot{v}^*(\xi, 0) &= 0 \\ \dot{v}_\xi^*(\xi, 0) &= 0 \end{aligned} \quad (109)$$

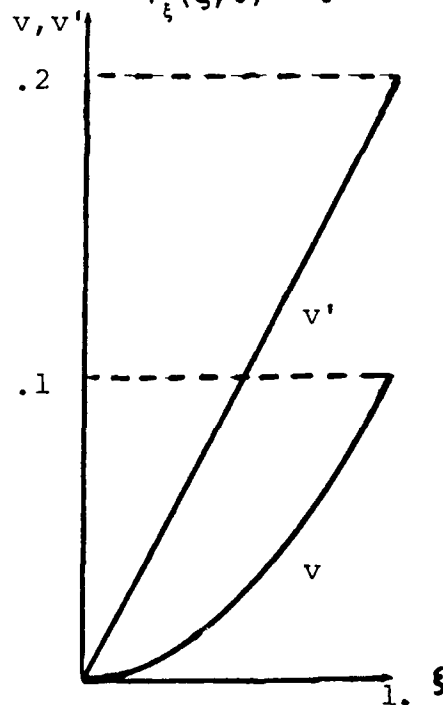


Figure 4.2 Parabolic and Linear Initial Conditions Plot Case Study One and Four

The prescribed functions of $L(t)$ and its velocity are,

$$L(t) = L_0 - .166t \quad (110)$$

$$\dot{L}(t) = -.166$$

The $L(t)$, function was constructed to permit the beam to be drawn half way (10 inches) into the sleeve (hole) in 60 seconds. Figure (4.3) is a plot of $L(t)$ and velocity, $\dot{L}(t)$.

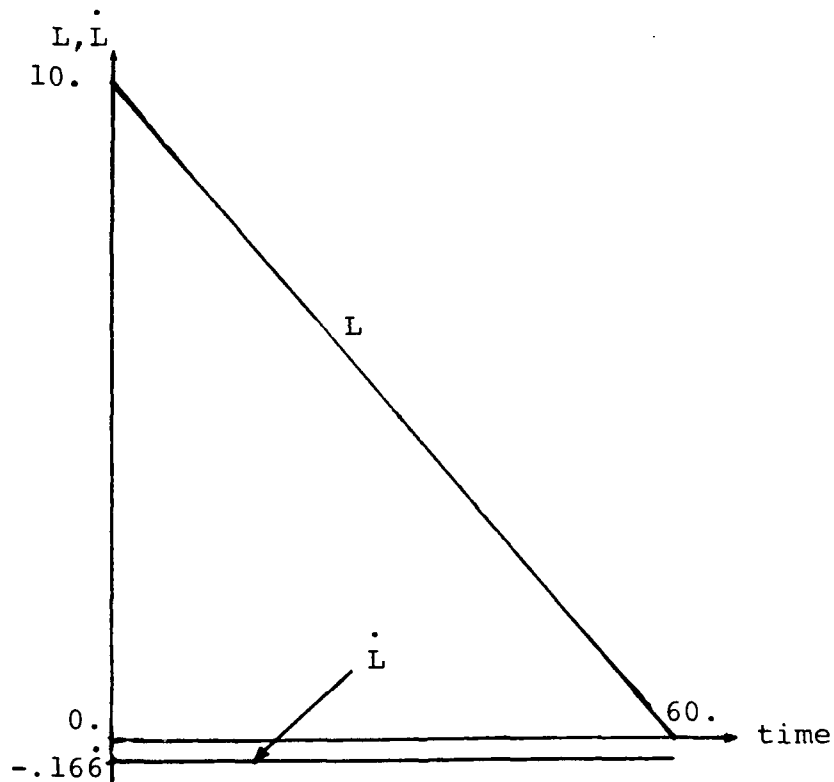


Figure 4.3 Length and Velocity Function Plot
Case Study One

This problem was solved for a four, eight, and sixteen element discretization. This was the only investigation of grid independence conducted. The results of this investigation were discussed in the subsection on spatial grid independence.

C. SECOND CASE STUDY, PARABOLIC FUNCTIONS OF $L(t)$

Two studies are conducted where $L(t)$ is prescribed by different parabolic functions. If $L(t)$ is defined as a parabolic function, its first and second derivatives are non zero and significant (See Figures 4.5 and 4.6). Thus, the system in Equation (99) is completely defined. In addition to the dissimilar functions of $L(t)$, the two cases are distinct in their cross-sectional geometries.

The same initial conditions were imposed for the two cases. An initial deformation of the beam in a parabolic shape was imposed again as in the first case study and again the initial velocities are zero. The λ vector of Equation (99) was initialized for all DOF according to the following displacements and slopes (See Figure 4.4),

$$\begin{aligned}v^*(\xi, 0) &= \xi^2 \\v_{\xi}^*(\xi, 0) &= 2\xi\end{aligned}\tag{111}$$

and velocities,

$$\dot{v}^*(\xi, 0) = 0 \quad (112)$$

$$\dot{v}_\xi^*(\xi, 0) = 0$$

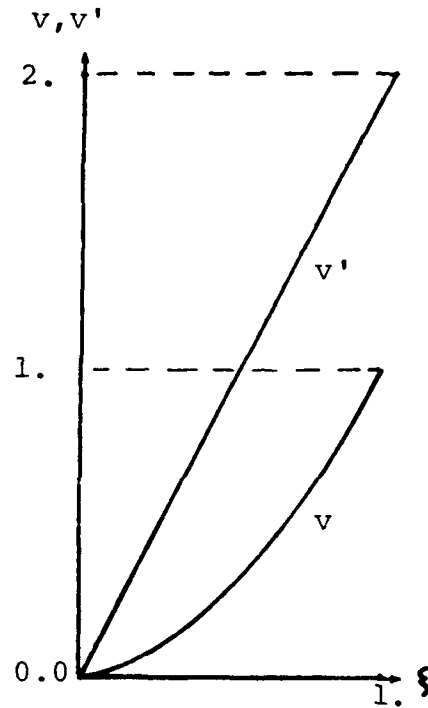


Figure 4.4 Parabolic and Linear Initial Conditions
Plots Case Study Two

1. Parabolic $L(t)$, The Less Stiff Beam

"Case One" of the second case study is the less "stiff" problem. Figure (4.1) shows the cross sectional dimensions. These dimensions result in material and geometric properties such that ρ (mass/unit length) = $3.493\text{E-}6 \text{ lbf} \cdot \text{S}^2/\text{in}^2$, and moment of inertia $I = 10.17\text{E-}6 \text{ in}^4$.

A parabolic function of $L(t)$ is prescribed such that the beam is drawn to half its original length in 2.5 seconds, reverses direction, and returns to its original length during the next 2.5 seconds, for a total of 5 seconds. Figure (4.5) is a plot of $L(t)$ and its derivatives, velocity and acceleration. The functions are,

$$\begin{aligned} L(t) &= L_0 - 4t + .8t^2 \\ \dot{L}(t) &= -4 + 1.6t & \{0 \leq t \leq 5.0\} \text{ sec.} & (113) \\ \ddot{L}(t) &= 1.6 \end{aligned}$$

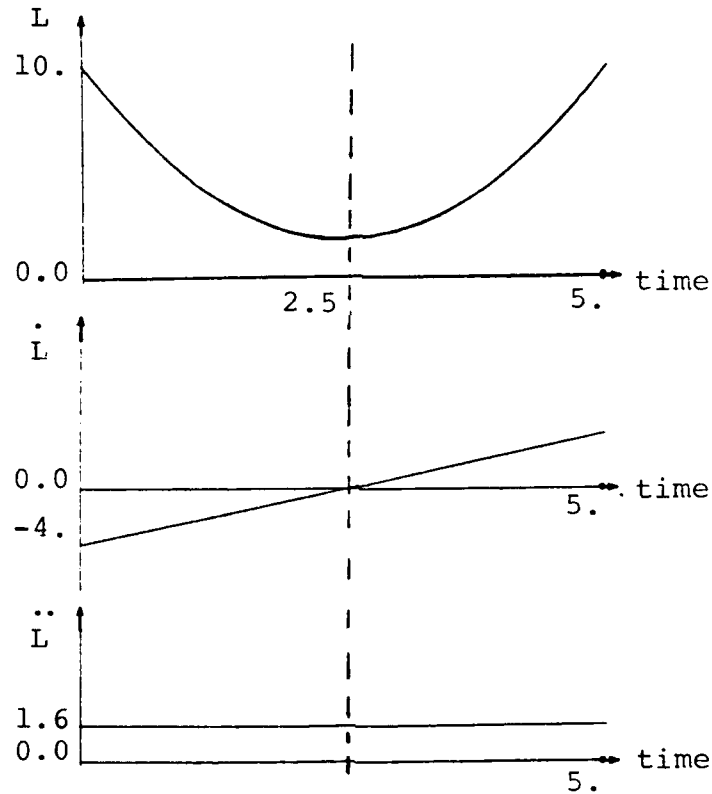


Figure 4.5 Length, Velocity, and Acceleration Plots
Case Study Two (Less Stiff Beam)

2. Parabolic $L(t)$, The Stiff Beam

"Case Two" of the second case study is the stiffer of the two parabolic $L(t)$ case studies. Figure (4.1) shows the cross sectional dimensions of the beam. These dimensions result in material and geometric properties such that ρ (mass/unit length) = $6.988\text{E-}6$ lbf·S²/in², and moment of inertia $I = 81.38\text{E-}6$ in⁴.

"Case Two" was started with the same parabolic function for $L(t)$ as "Case One". It was here that the significance of "stiffness" and computational time came to focus. Running the two cases simultaneously as separate jobs on different system accounts, clearly demonstrated the difference in CPU requirements for the two problems. In fact, there was such a disparity in computational effort that it was decided to change the course of the stiffer problem ("Case Two") such that it's symmetric, cycle would be complete in 2.1 seconds vice the 5 seconds of "Case One". The functions of $L(t)$ and their derivatives, along with their respective time domains are given here,

$$L(t) = L_0 - 4t + .8t^2$$

$$\dot{L}(t) = -4 + 1.6t \quad \{0 \leq t \leq 1.0\} \text{ sec.}$$

$$\ddot{L}(t) = 1.6$$

$$L(t) = 33.2 - 50.4t + 24t^2$$

$$\dot{L}(t) = -50.4 + 48t \quad \{1.0 \leq t \leq 1.1\} \text{ sec.}$$

$$\ddot{L}(t) = 48.0$$

$$L(t) = 5.128 + .64t + .8t^2$$

$$\dot{L}(t) = .64 + 1.6t \quad \{1.1 \leq t \leq 2.1\} \text{ sec.}$$

$$\ddot{L}(t) = 1.6$$

These functions are plotted below in Figure (4.6).

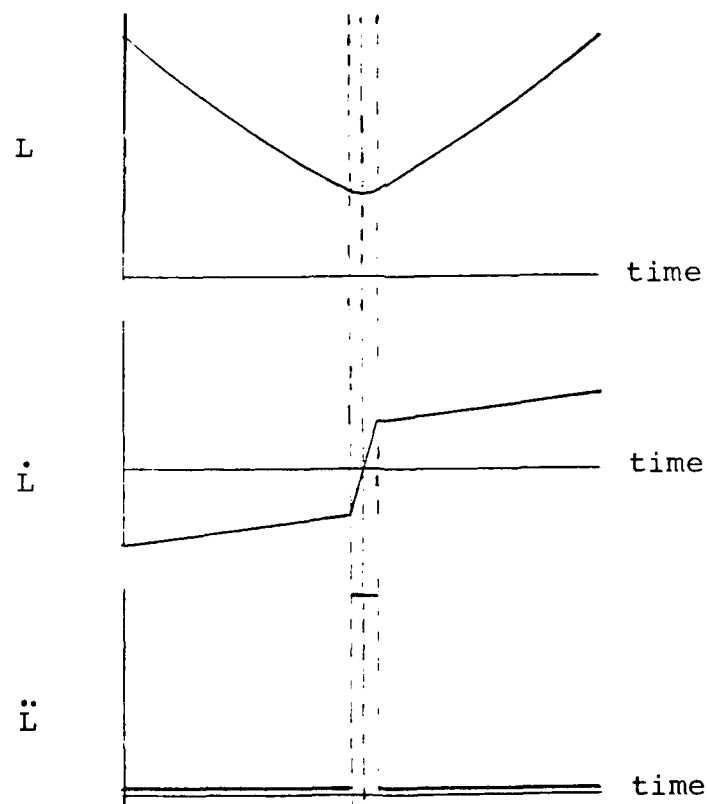


Figure 4.6 Length, Velocity, and Acceleration Function Plots
Case Study Two (Stiff Beam)

3. Discussion of the Parabolic Cases

The results of these runs provided one of the thought provoking questions of the research. The purpose behind the parabolic function of $L(t)$ was to observe the beam's activity in the case where it returned to its original length in a symmetric, cyclic fashion. The interest was in the question, would the expected symmetric behavior of the 'pull-push' sequence of $L(t)$ be predicted by the code? The results clearly showed that symmetry did not occur for the parabolic cases (See Figures (4.10) and (4.11)). In fact, the deflections had grown considerably during the 'push' stage of the $L(t)$ cycle. Where did the energy to cause such large deflections come from? One possible explanation considered was that through the imposition of $L(t)$, energy in the form of work had been added to the system. This question was addressed in the final case study, wherein the work associated with $\int FdL$ was tracked. Another possibility, if the work cannot account for the increase in displacements, is that the results are not correct due to a break down in the numerical integration during the latter stage of the 'push' stage of the cycle.

Before continuing on to the next set of case studies, a discussion of what is a most thought provoking question resulting from the research thus far follows. What would happen if the beam were drawn totally through the

frictionless hole and then pushed back out to its original length? At the end of the 'pull' stage of the cycle, the entire beam resides motionless in a straight sleeve (the frictionless hole) and therefore there is neither deformational (strain) energy or vibrating (kinetic) energy. Again, energy transfer out of the system as work could account for this phenomena. In any case, it may not be possible to show this with this numerical model for the following reasons. For one thing, as the length of the beam shortens, the shear and rotary inertia terms, which were not included in this model, become ever increasingly significant and in fact may dominate the physical behavior. Secondly, even if the physical model could be modified to include these effects, the frequencies tend toward infinity as $L(t)$ approaches zero, and numerical integration would not be possible.

D. HARMONIC $L(t)$ PRESCRIBED

Two studies were conducted simultaneously on two beams with the material and geometric properties identical to the two beams used in the parabolic $L(t)$ study. In this study, $L(t)$ was prescribed as the trigonometric functions of $L(t)$ and

its derivatives given here,

$$L(t) = 9 + \cos\left(\frac{\pi t}{1.5}\right)$$

$$\dot{L}(t) = -\frac{\pi}{1.5} \sin\left(\frac{\pi t}{1.5}\right) \quad \{0 \leq t \leq 3.0\} \text{ sec.} \quad (116)$$

$$\ddot{L}(t) = -\left(\frac{\pi}{1.5}\right)^2 \cos\left(\frac{\pi t}{1.5}\right)$$

Accordingly, $L(t)$ for these cases varied between eight and ten inches (Fig. 4.7). The symmetric, cyclic concept was used again as it was in the parabolic $L(t)$ prescribed cases.

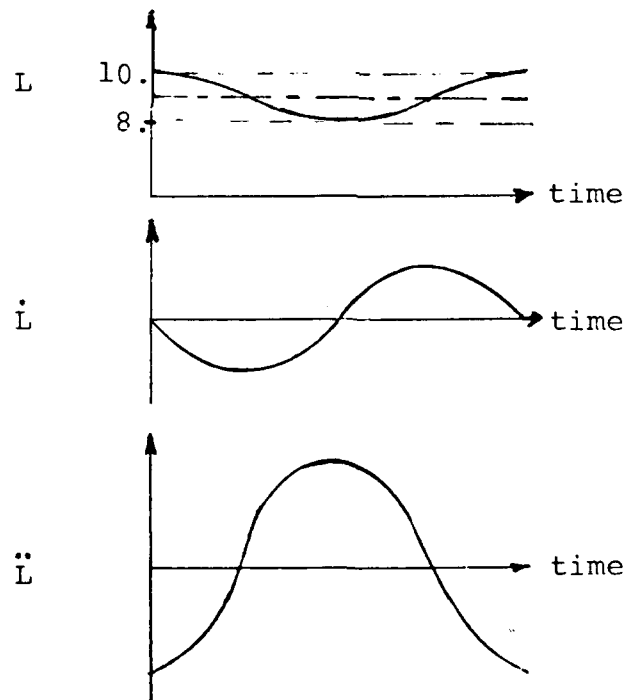


Figure 4.7 Length, Velocity, and Acceleration Function Plots
Case Study Three (Both Beams)

A sinusoidal function was also prescribed for the initial deformation of the 10 inch plexiglass beam. The λ vector was initialized for all DOF in accordance with the following displacements and slopes,

$$\begin{aligned} v^*(\xi, 0) &= 0.1 \left[1 - \cos\left(\frac{\pi\xi}{2.0}\right) \right] \\ v_{\xi}^*(\xi, 0) &= \frac{\pi}{20.0} \sin\left(\frac{\pi\xi}{2.0}\right) \end{aligned} \quad (117)$$

and velocities,

$$\begin{aligned} \dot{v}^*(\xi, 0) &= 0 \\ \dot{v}_{\xi}^*(\xi, 0) &= 0 \end{aligned} \quad (118)$$

The initial conditions on deflection and slope are shown graphically in Figure (4.8).

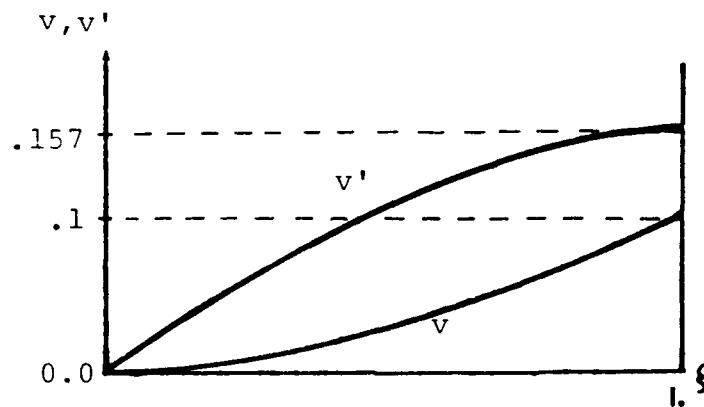


Figure 4.8 Sinusoidal Initial Conditions Plot

The previous results of increasing displacements (above the initial displacements) observed for the parabolic $L(t)$ studies were not obtained in these harmonic $L(t)$ case studies (See Figures (4.12) and (4.13)). If the work explanation is the correct one in the previous section, then it might be that work is associated with parabolic $L(t)$ axial motions, and not with harmonic $L(t)$ axial motions. In order to investigate this question further, a investigation was undertaken to track work for the parabolic $L(t)$ case. This is discussed in the next section. The computational effort observations of the previous cases were noted again as well. That is, the CPU requirement for the "stiffer" problem was greater than for the "less stiff" problem, as it had been for the parabolic $L(t)$ cases.

E. CASE STUDY FOUR, TRACKING WORK FOR A PARABOLIC $L(t)$

A final study was conducted using the "less stiff" beam in which a parabolic $L(t)$ was prescribed. The function and its derivatives follow and are plotted in Figure (4.9).

$$L(t) = 10.0 - 2.666t + .888t^2$$

$$\dot{L}(t) = 2.666 + 1.777t \quad \{0 \leq t \leq 3.0\} \text{ sec.}$$

$$\ddot{L}(t) = 1.777$$

The λ vector was initialized for all DOF according to the initial deformation of the beam defined by the following displacements and slopes,

$$\begin{aligned} v^*(\xi, 0) &= .1\xi^2 \\ v_\xi^*(\xi, 0) &= .2\xi \end{aligned} \quad (120)$$

and velocities,

$$\begin{aligned} \dot{v}^*(\xi, 0) &= 0 \\ \dot{v}_\xi^*(\xi, 0) &= 0 \end{aligned} \quad (121)$$

These are the same initial conditions as used in the first Case Study and are plotted in Figure (4.2).

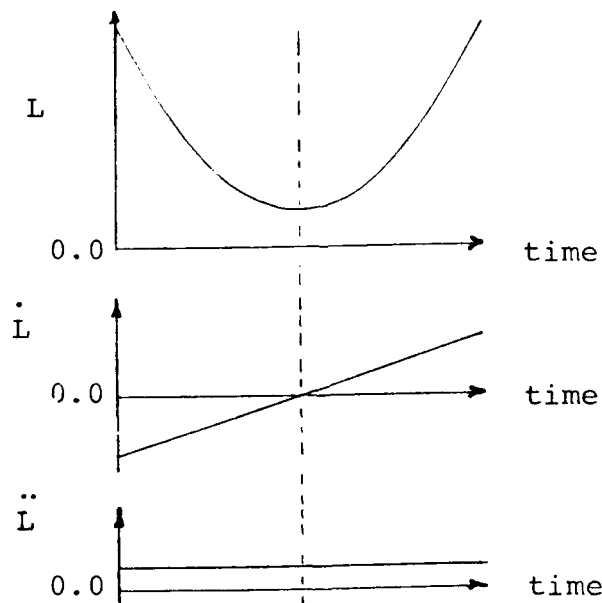


Figure 4.9 Length, velocity, and Acceleration Plots
Case Study Four

The purpose of this final study was to determine whether the increased displacements predicted by the code for the parabolic $L(t)$ cases, during the latter stages of the 'push' stage of the cycle, could be accounted for by work input to the system. In addition to tracking work, the moment and shear were also tracked. The shear diagrams, shown in Figures (4.15) to (4.17), and moment diagrams, shown in Figures (4.18) to (4.20), appear to be reasonable. The small values of these parameters is due to the values of Young's modulus, E , and moment of inertia, I , used in this study. The product of EI for the cases studies here are 1.017 lb. in², and 8.138 lb. in².

The diagrams for axial force F and work W , shown in Figure (4.21) do not appear to be reasonable and therefore are suspect. Assuming a one to one relation between $L(t)$ and $F(t)$ exists, it is difficult to imagine that such a force would produce the smooth parabolic $L(t)$ and vice versa. A tentative conclusion therefore is that either $F(t)$ was not coded correctly or that there is in fact an instability in the numerical integration during the latter stage of the 'push' cycle of the problem. An effort is presently underway to determine if the coding for the calculation of $F(t)$ is correct. It should be remarked however that prior to the erratic behavior of $F(t)$, which occurs late in the 'pull-push' cycle, the values of $F(t)$ seemed reasonable.

F. FINAL COMMENTS AND RECOMMENDATIONS

The results of this initial investigation on the behavior of a vibrating beam subject to a prescribed axial motion leads to the following conclusions. First and foremost is that the implementation of the FEM numerical scheme was accomplished with success, although it is not certain that some numerical difficulties are not encountered at the later stages of the analysis. Further work must be undertaken to resolve whether the increase in vibration amplitude which is predicted by the code is an actual result of work input to the system or whether it is associated with a numerical instability. Prior to the investigation of the 'real' gun barrel problem, One might also investigate whether the omission of axial strain energy from the model, which is common whenever bending and bar activity coexists, could account for this behavior. If so, additional terms for axial strain energy could be included in the formulation.

It is interesting to note that the equation of axial motion relates the axial force $F(t)$ not only to the axial acceleration \ddot{L} , in accordance with Newton's law of motion for rigid bodies, but also includes additional terms associated with the deformational strain energy of bending, and the kinetic energy of beam vibration, at the free end of the beam. The former term adds to the acceleration term while the latter term decreases it.

The practical problem associated with the axial motion of a gun barrel due to the recoil action of firing, which provided the impetus for this study, was formulated but not solved here. An experimental investigation should be undertaken to ascertain the accuracy of the numerical model.

PARABOLIC AXIAL MOTION

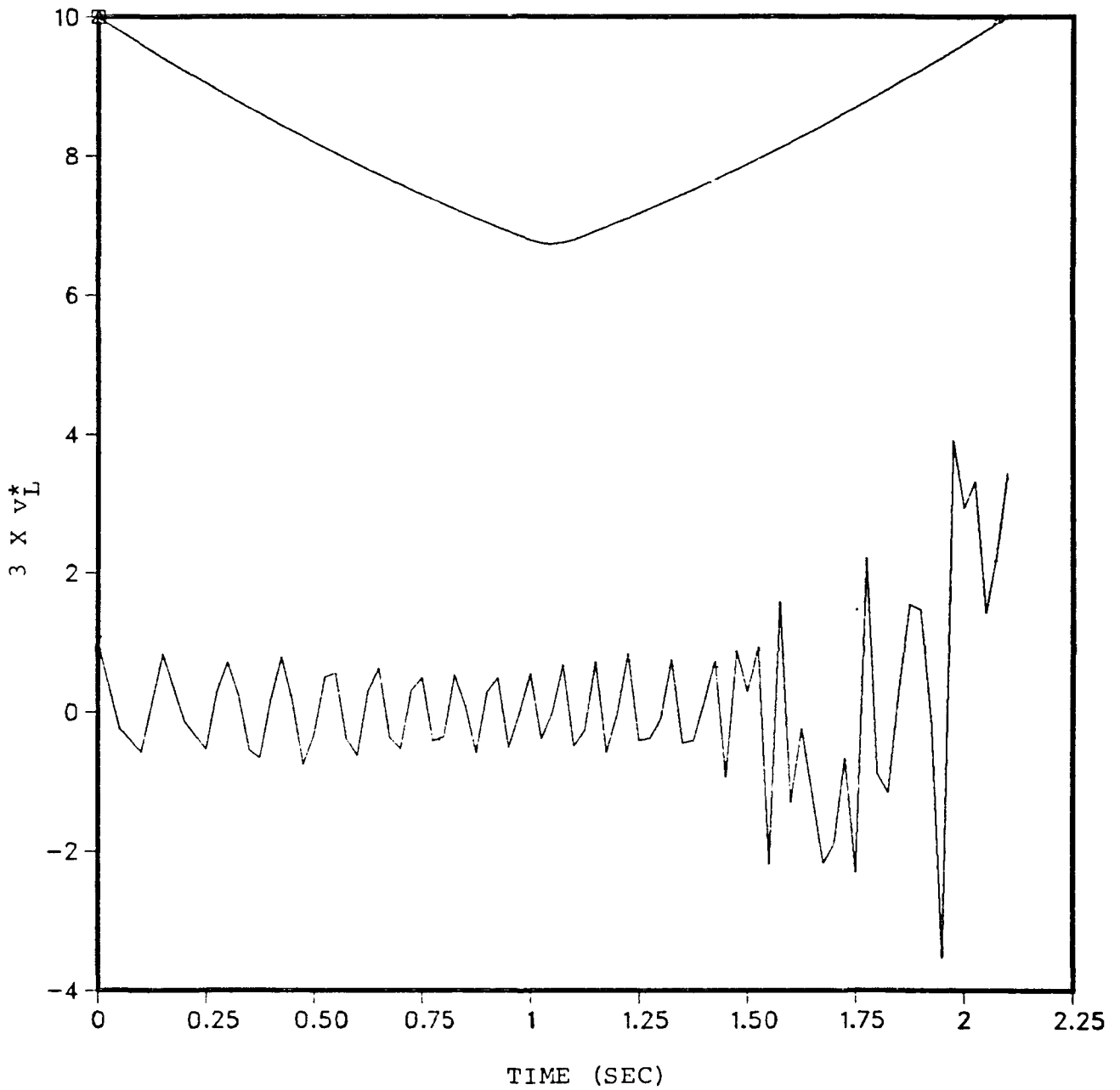


Figure 4.10 Parabolic Axial Motion Transient Response
Case Study Two (Stiff Beam)

PARABOLIC AXIAL MOTION

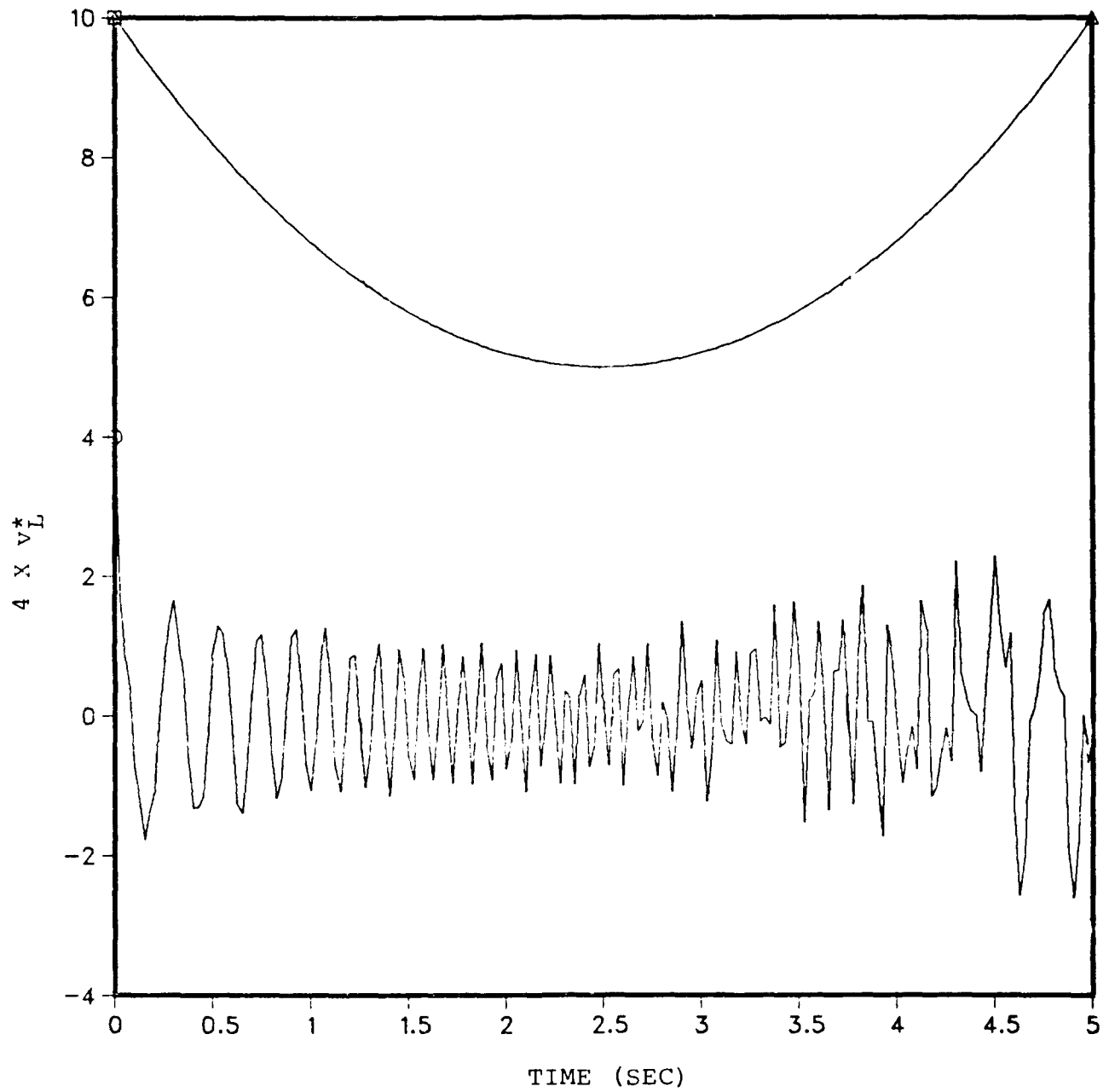


Figure 4.11 Parabolic Axial Motion Transient Response
Case Study Two (Less Stiff Beam)

HARMONIC AXIAL MOTION

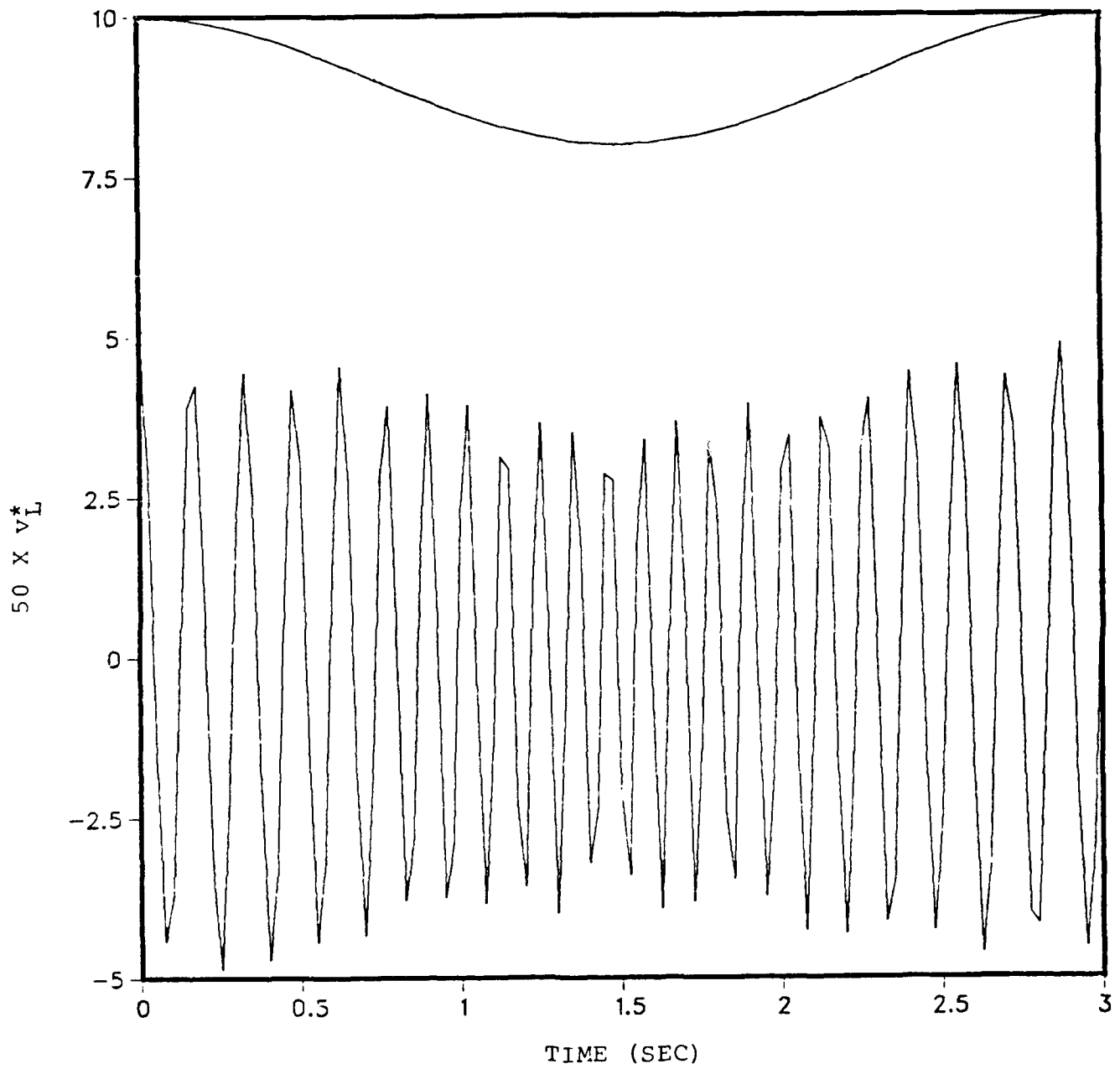


Figure 4.12 Harmonic Axial Motion Transient Response
Case Study Three (Stiff Beam)

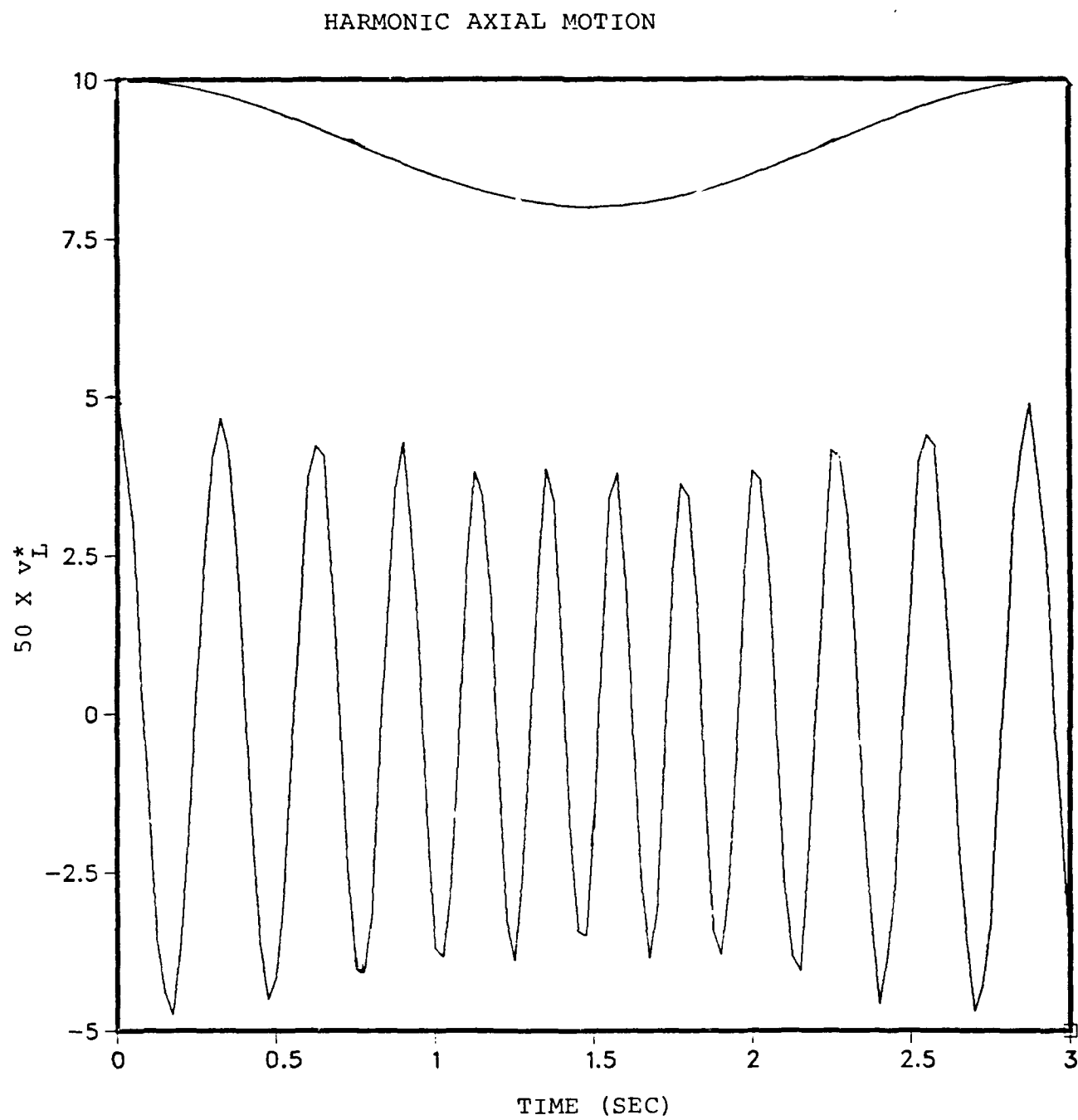


Figure 4.13 Harmonic Axial Motion Transient Response
Case Study Three (Less Stiff Beam)

PARABOLIC AXIAL MOTION

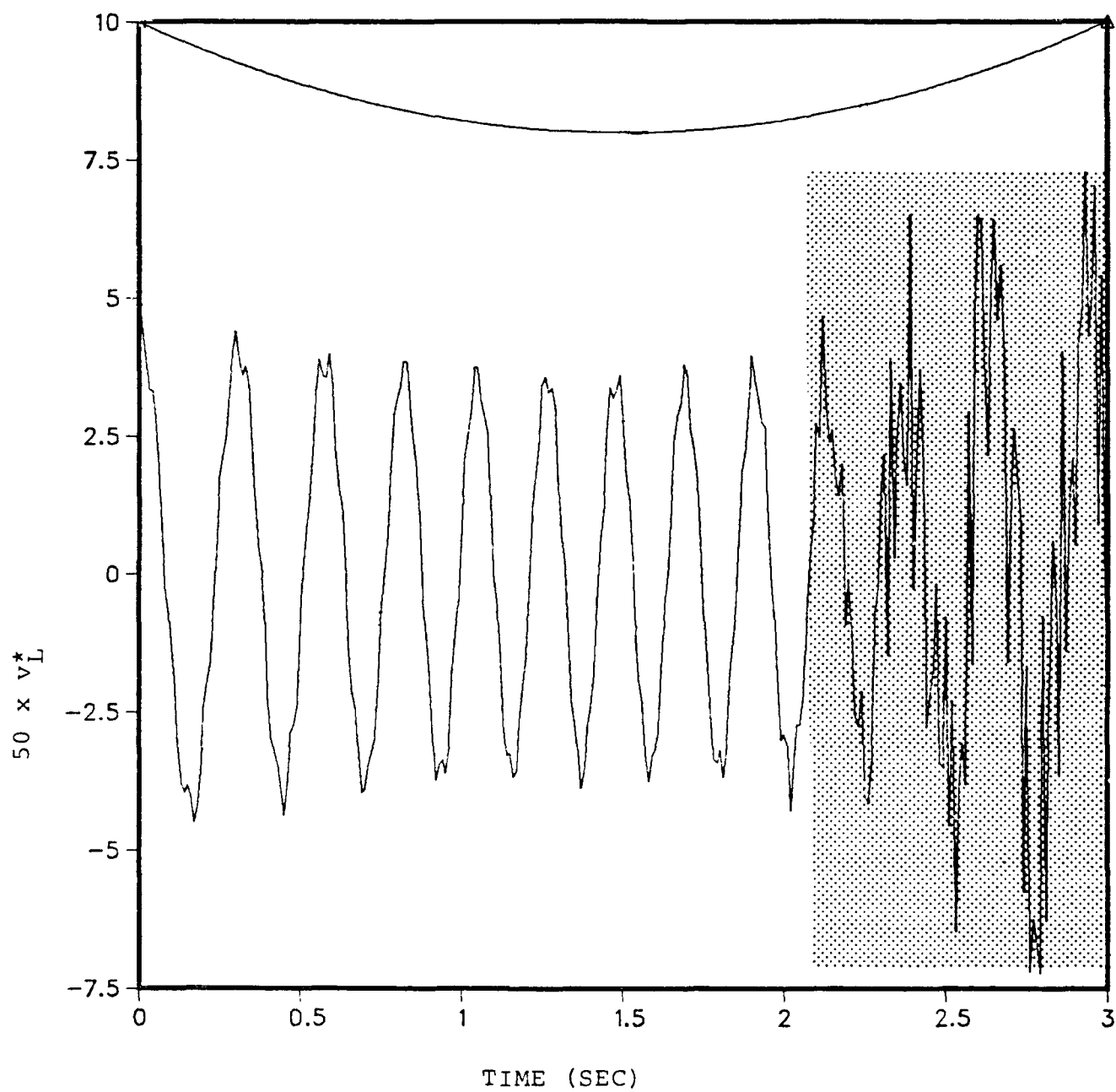


Figure 4.14 Parabolic Axial Motion Transient Response
Case Study Four

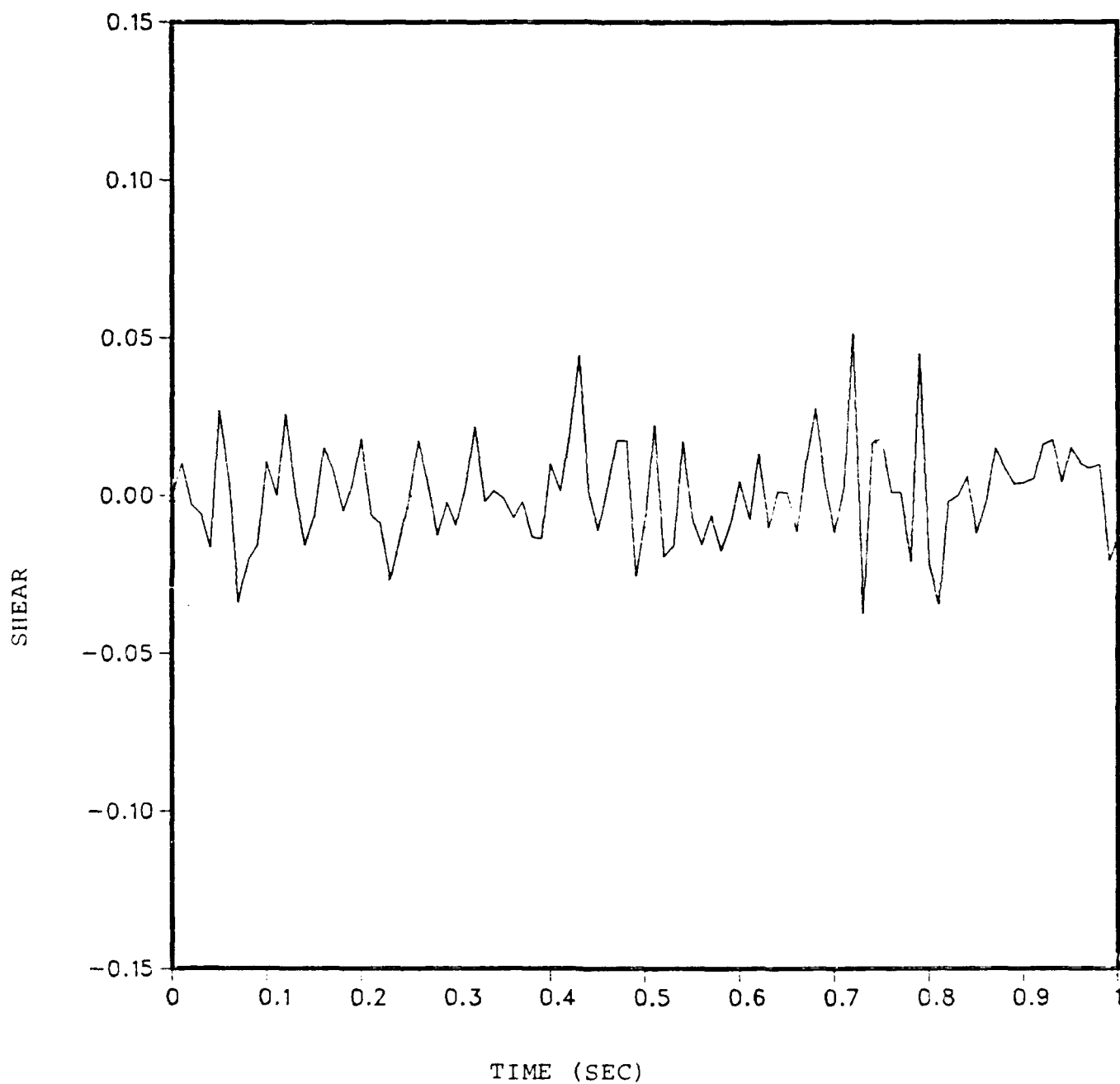


Figure 4.15 Shear Plot (0.0 - 1.0 Seconds)

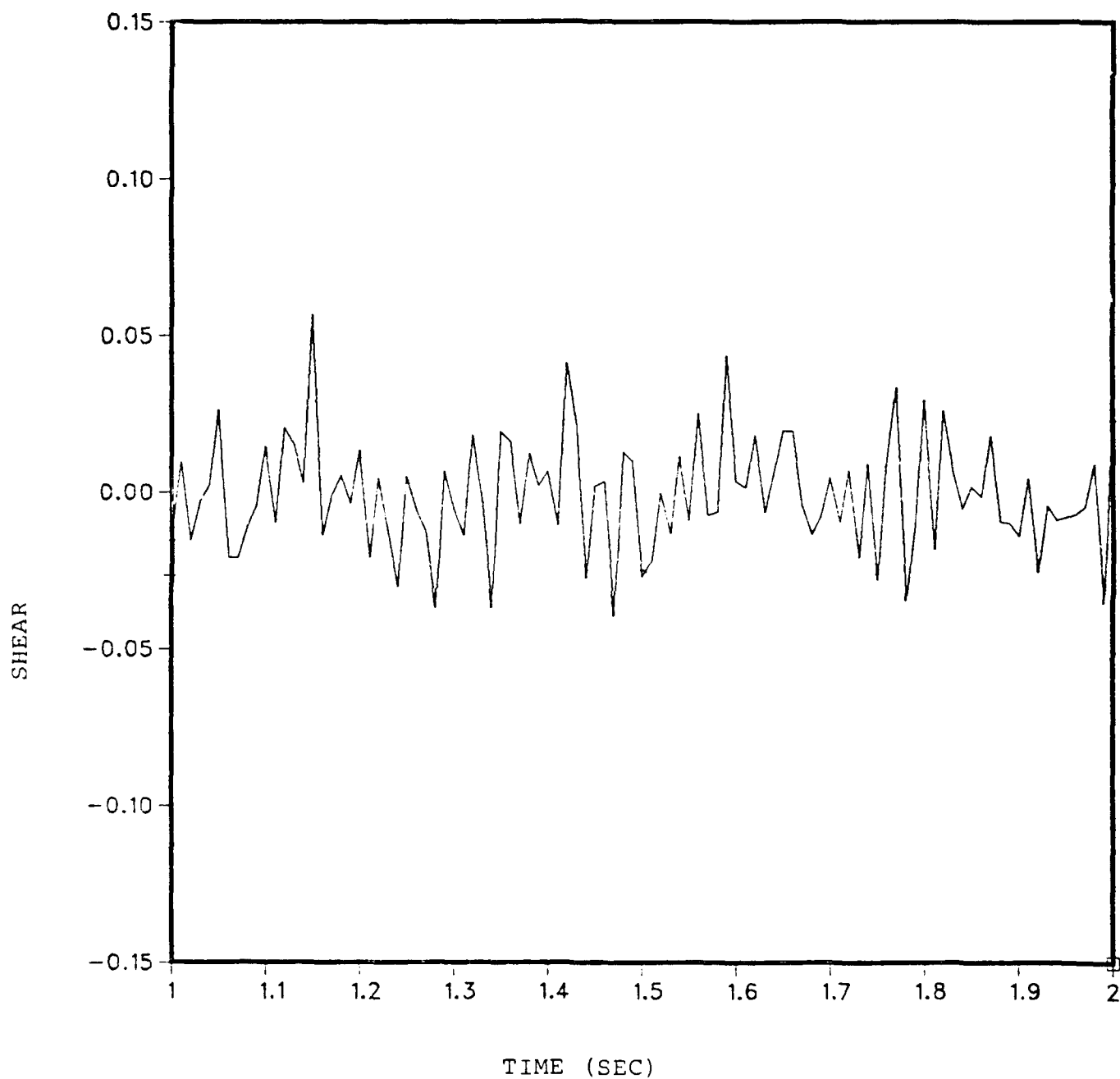


Figure 4.16 Shear Plot (1.0 - 2.0 Seconds)

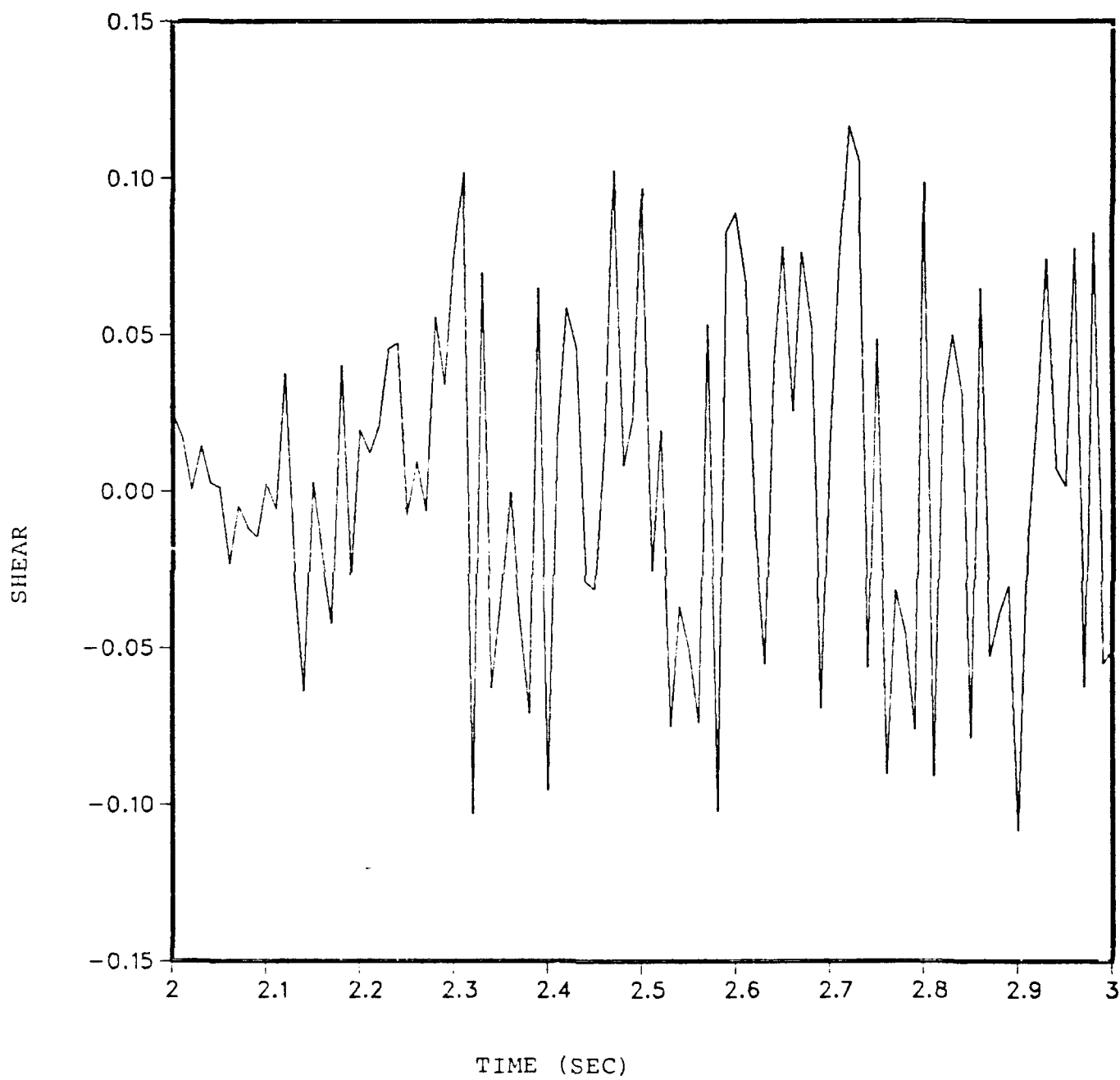


Figure 4.17 Shear Plot (2.0 - 3.0 Seconds)

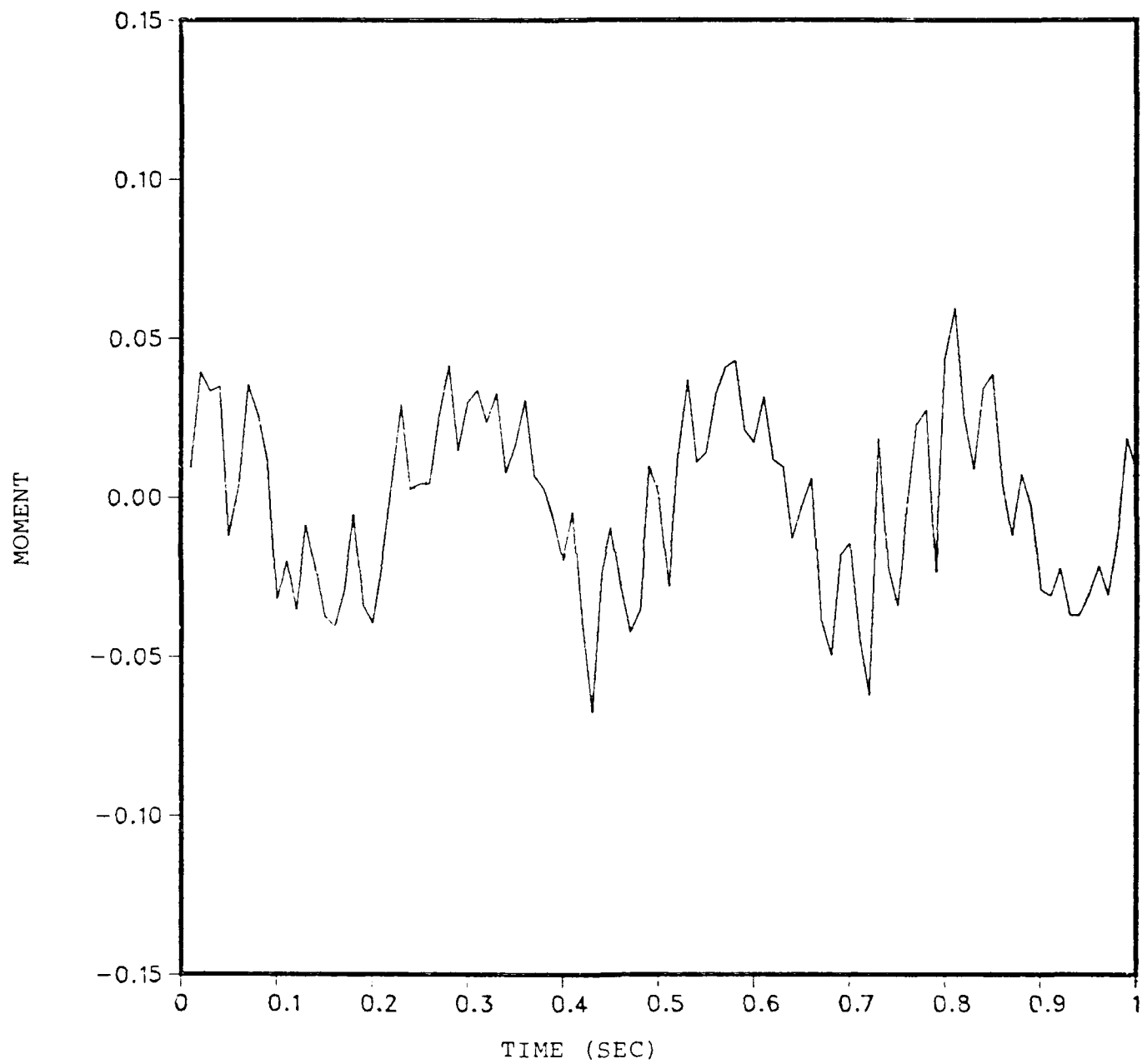


Figure 4.18 Moment Plot (0.0 - 1.0 Seconds)

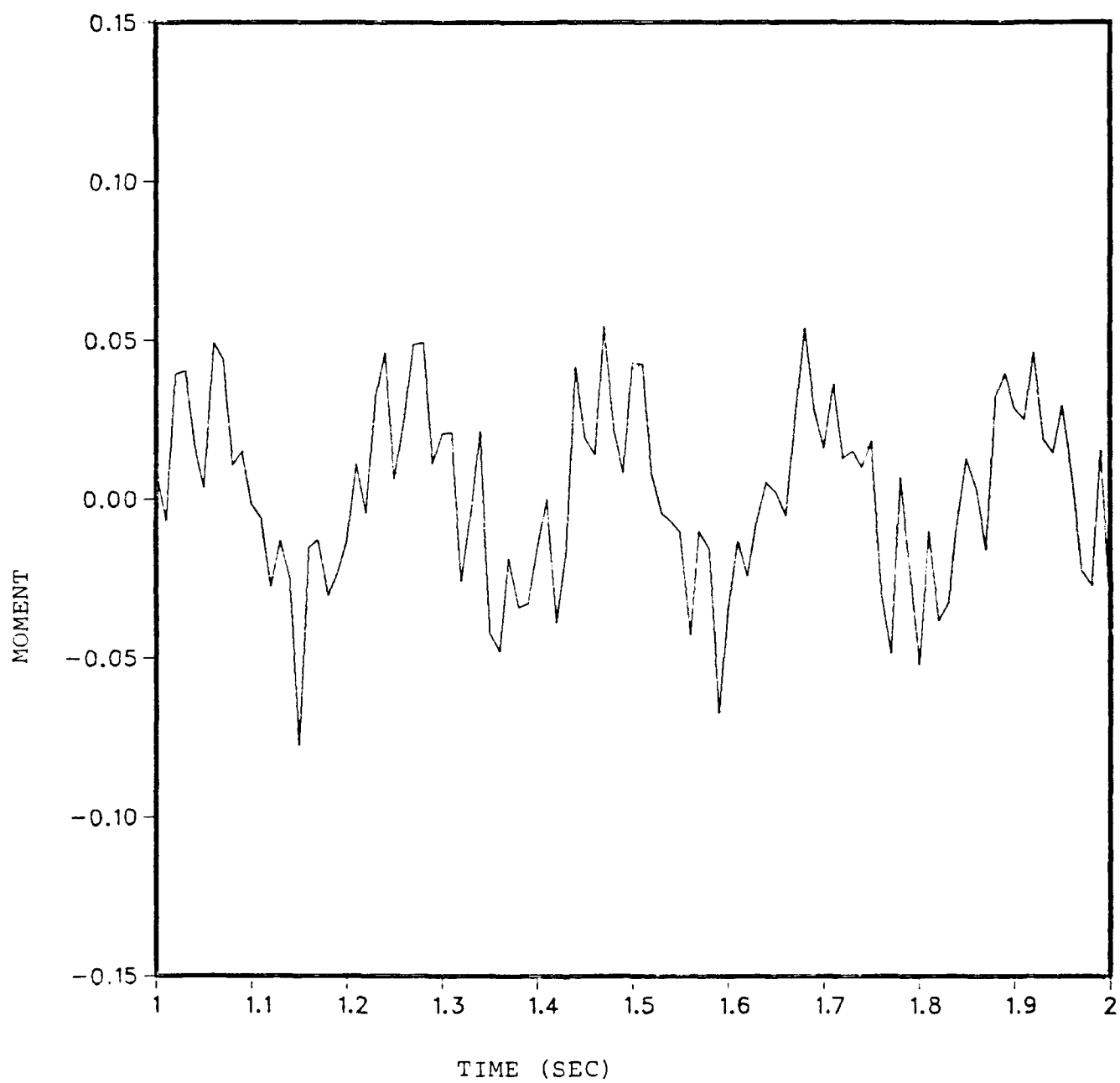


Figure 4.19 Moment Plot (1.0 - 2.0 Seconds)

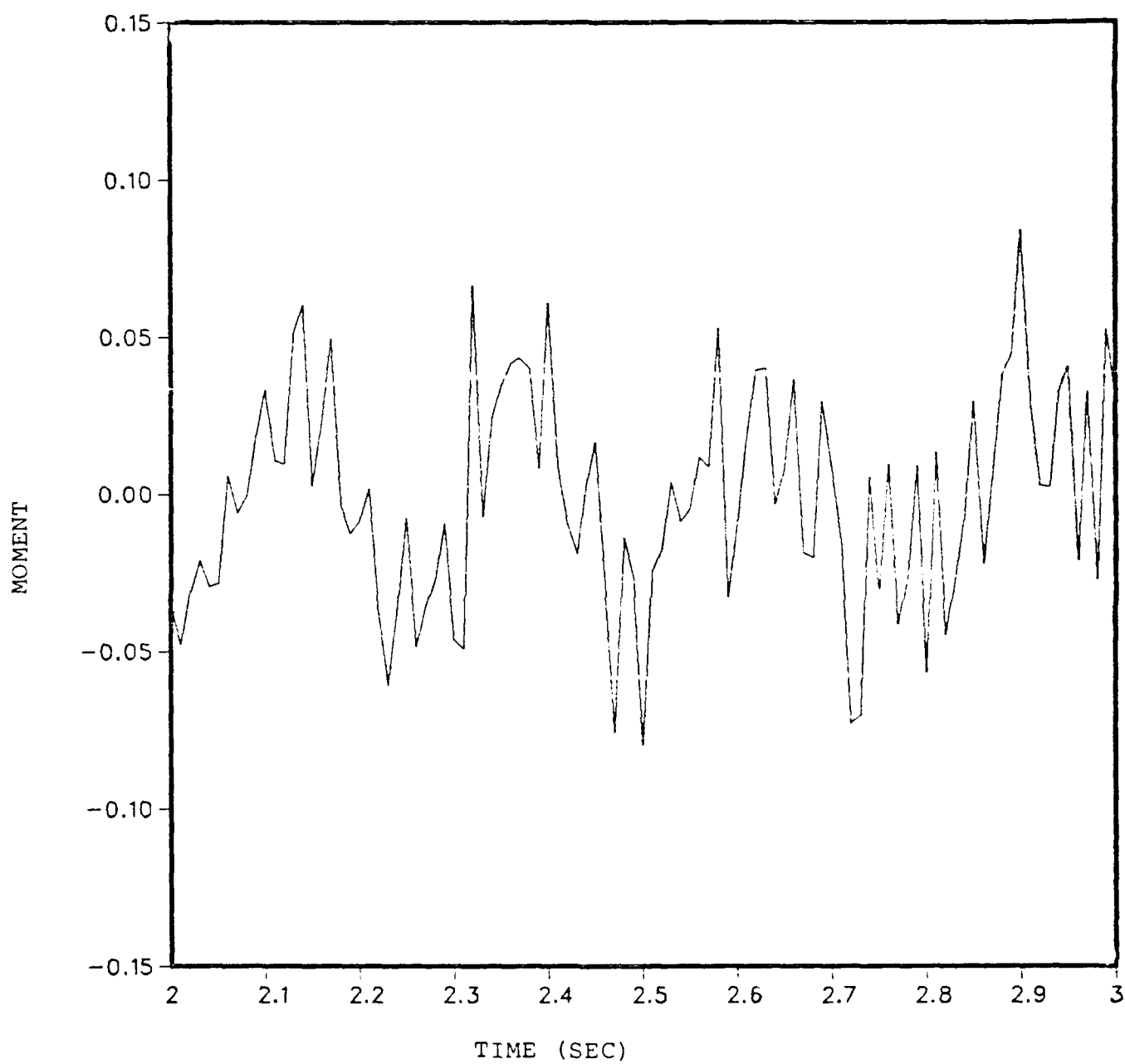


Figure 4.20 Moment Plot (2.0 - 3.0 Seconds)

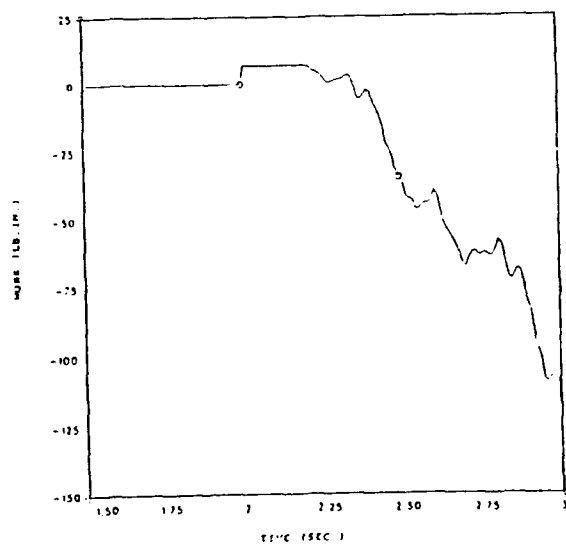
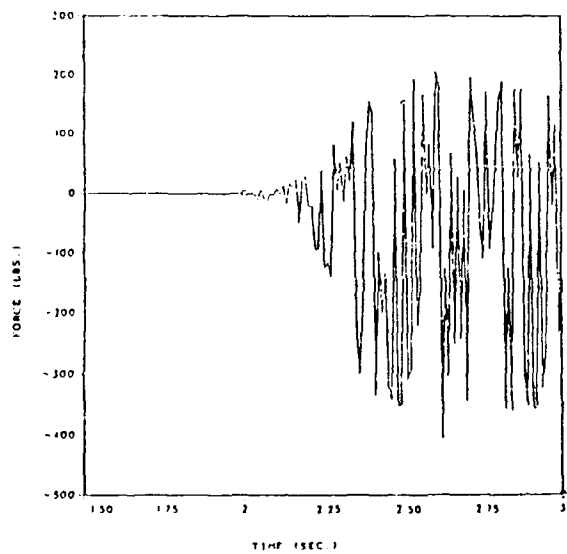
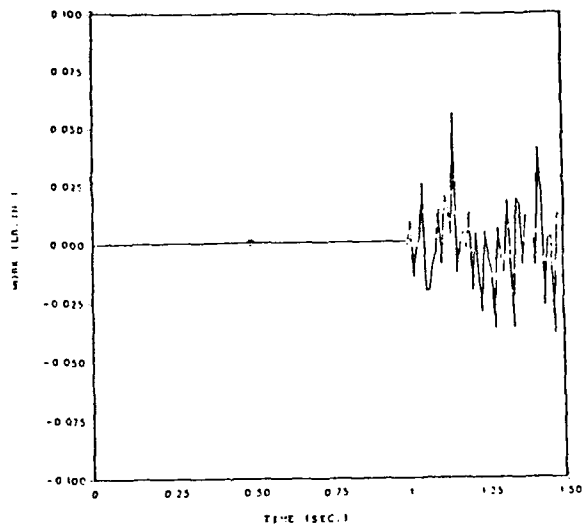
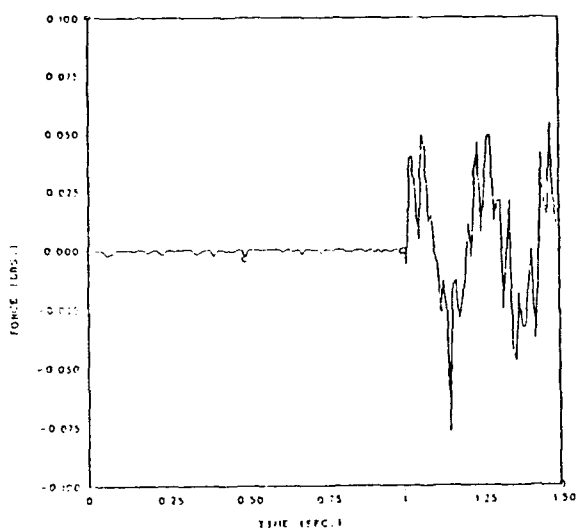
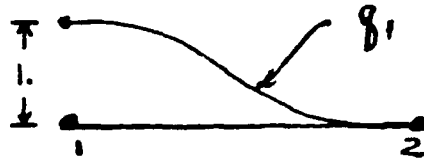


Figure 4.21 Force and Work Plots

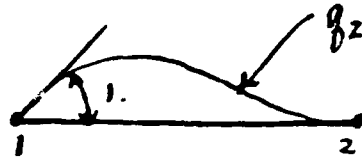
APPENDIX A THE CUBIC SPLINE SHAPE FUNCTIONS

The beam element is constructed using four shape functions (q_1 , q_2 , q_3 , and q_4) which satisfy the following conditions.



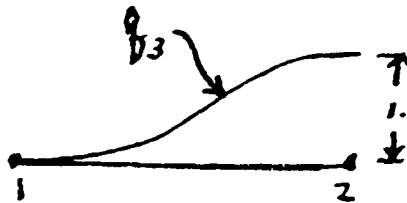
$$q_1(NP1) = 1 \quad , \quad q_1'(NP1) = 0$$

$$q_1(NP2) = 0 \quad , \quad q_1'(NP2) = 0$$



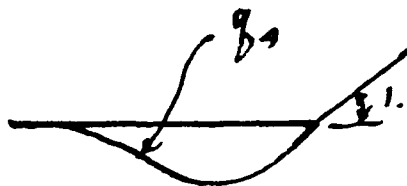
$$q_2(NP1) = 0 \quad , \quad q_2'(NP1) = 1$$

$$q_2(NP2) = 0 \quad , \quad q_2'(NP2) = 0$$



$$q_3(NP1) = 0 \quad , \quad q_3'(NP1) = 0$$

$$q_3(NP2) = 1 \quad , \quad q_3'(NP2) = 0$$



$$q_4(NP1) = 0 \quad , \quad q_4'(NP1) = 0$$

$$q_4(NP2) = 0 \quad , \quad q_4'(NP2) = 1$$

where the (') superscript represents a differentiation with respect to the spatial variable.

By satisfying the four conditions on each q_i , the four element shape functions can be constructed from a cubic equation of the form,

$$q_i = a_i + b_i \alpha + c_i \alpha^2 + d_i \alpha^3$$

q_1 is constructed here as an example.

$$q_1 = a_1 + b_1 \alpha + c_1 \alpha^2 + d_1 \alpha^3$$

$$1. \quad q_1(NP1) = 1 \Rightarrow 1 = a_1$$

$$2. \quad q_1'(NP1) = 0 \Rightarrow 0 = b_1$$

\Downarrow

$$q_1 = 1 + c_1 \alpha^2 + d_1 \alpha^3$$

\Downarrow

$$3. \quad q_1(NP2) = 0 \Rightarrow 0 = 1 + c_1 l_*^2 + d_1 l_*^3$$

$$4. \quad q_1'(NP2) = 0 \Rightarrow 0 = 2c_1 l_* + 3d_1 l_*^2 \Rightarrow c_1 = -\frac{3}{2}d_1 l_*$$

$$\text{substitute (4.)} \rightarrow (3.) \Rightarrow d_1 = \frac{2}{l_*^3} \text{ and, } c_1 = -\frac{3}{l_*^2}$$

thus,

$$q_1 = 1 - \frac{3}{l_*^2} \alpha^2 + \frac{2}{l_*^3} \alpha^3$$

Using the conditions which define shape functions q_2 , q_3 , and, q_4 (listed on the previous page) the other three shape functions are obtained,

$$q_2 = \alpha - \frac{2}{l_*} \alpha^2 + \frac{1}{l_*^2} \alpha^3$$

$$q_3 = \frac{3}{l_*^2} \alpha^2 - \frac{2}{l_*^3} \alpha^3$$

$$q_4 = -\frac{1}{l_*} \alpha^2 + \frac{1}{l_*^2} \alpha^3$$

APPENDIX B **CONSTRUCTION OF THE GLOBAL MATRICES**

The global matrices **A**, **B**, **C**, and, **D** are constructed from the element matrices **a**^{*}, **b**^{*}, **c**^{*}, and, **d**^{*} according to relationships;

$$\begin{aligned}
 \mathbf{A} &= \int_0^1 \mathbf{Q}'' (\mathbf{Q}^T)'' d\xi = \mathbf{U} \mathbf{a}^* \\
 \mathbf{B} &= \int_0^1 \xi^2 \mathbf{Q} (\mathbf{Q}^T)'' d\xi = \mathbf{U} \mathbf{b}^* \\
 \mathbf{C} &= \int_0^1 \xi \mathbf{Q} (\mathbf{Q}^T)' d\xi = \mathbf{U} \mathbf{c}^* \\
 \mathbf{D} &= \int_0^1 \mathbf{Q} (\mathbf{Q}^T)' d\xi = \mathbf{U} \mathbf{d}^*
 \end{aligned}
 \tag{129}$$

where,

$$\begin{aligned}
 \mathbf{a}^* &= \int_{1_1} \mathbf{q}'' (\mathbf{q}^T)'' d\alpha \\
 \mathbf{b}^* &= \bar{\xi}^2 \int_{1_1} \mathbf{q} (\mathbf{q}^T)'' d\alpha \\
 \mathbf{c}^* &= \bar{\xi} \int_{1_1} \mathbf{q} (\mathbf{q}^T)' d\alpha \\
 \mathbf{d}^* &= \int_{1_1} \mathbf{q} (\mathbf{q}^T)' d\alpha
 \end{aligned}
 \tag{130}$$

given that $\bar{\xi}$ is a constant which approximates ξ transformed to the local coordinate α .

The transformation of ξ is as follows. Referring to Figure (B.1),

$$\xi = \alpha + \eta_n \quad \text{where, } \eta_n = \sum_{j=1}^{n-1} l_j,$$

$$\text{and, } \xi^2 = \alpha^2 + 2\eta_n \alpha + \eta_n^2$$

Because the transformation of ξ to a function of α results in integrals which are difficult to evaluate, it is desirable to use an alternative strategy. If we let,

$$\xi \approx \bar{\xi} = \eta_n + \frac{l_n}{2}$$

a numeric value can be assigned to this quantity. Thus, the difficult integration is eliminated. Any accuracy lost in the approximation will be recovered by additional iterations to obtain convergence of the FEM solution.

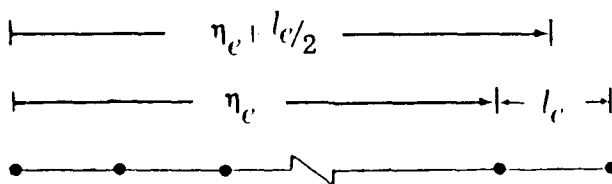


Figure B.1

The final \mathbf{a}^* , \mathbf{b}^* , \mathbf{c}^* , and, \mathbf{d}^* matrices follow,

$$\mathbf{a}^* = \begin{bmatrix} \frac{12}{l_1^3} & \frac{6}{l_1^2} & -\frac{12}{l_1^3} & \frac{6}{l_1^2} \\ \frac{6}{l_1^2} & \frac{4}{l_1} & -\frac{6}{l_1^2} & \frac{2}{l_1} \\ -\frac{12}{l_1^2} & -\frac{6}{l_1} & \frac{12}{l_1^3} & -\frac{6}{l_1^2} \\ \frac{6}{l_1^2} & \frac{2}{l_1} & -\frac{6}{l_1^2} & \frac{4}{l_1} \end{bmatrix}$$

$$\mathbf{b}^* = \bar{\xi}^2 \begin{bmatrix} -\frac{6}{5l_1} & -\frac{11}{10} & \frac{6}{5l_1} & -\frac{1}{10} \\ -\frac{1}{10} & -\frac{2l_1}{15} & \frac{1}{10} & \frac{l_1}{30} \\ \frac{6}{5l_1} & \frac{1}{10} & -\frac{6}{5l_1} & \frac{11}{10} \\ -\frac{1}{10} & \frac{l_1}{30} & \frac{1}{10} & -\frac{2l_1}{15} \end{bmatrix}$$

$$c^* = \bar{\xi} \begin{bmatrix} -\frac{1}{2} & \frac{1}{10} & \frac{1}{2} & -\frac{1}{10} \\ -\frac{1}{10} & 0 & \frac{1}{10} & -\frac{1^2}{60} \\ -\frac{1}{2} & -\frac{1}{10} & \frac{1}{2} & \frac{1}{10} \\ \frac{1}{10} & \frac{1^2}{60} & -\frac{1}{10} & 0 \end{bmatrix}$$

$$d^* = \begin{bmatrix} \frac{131}{35} & \frac{111^2}{210} & \frac{91}{70} & -\frac{131^2}{420} \\ \frac{111^2}{210} & \frac{1^3}{105} & \frac{131^2}{420} & -\frac{1^3}{140} \\ \frac{91}{70} & \frac{131^2}{420} & \frac{131}{35} & -\frac{111^2}{210} \\ -\frac{131^2}{420} & -\frac{1^3}{140} & -\frac{111^2}{210} & \frac{1^3}{105} \end{bmatrix}$$

APPENDIX C **STATIC CANTILEVER BEAM FORTRAN CODE** **AND SAMPLE OUTPUT**

```

*****
*                               MARK R. DEVRIES LT USCG
*                               NAVAL POSTGRADUATE SCHOOL
*                               SEPTEMBER 1990
*                               THESIS
* MASTER OF SCIENCE IN MECHANICAL ENGINEERING
*
*                               TITLE:
* VIBRATION OF A CANTILEVER BEAM
* THAT SLIDES AXIALLY IN A FRICTIONLESS HOLE
*
* THE FOLLOWING FORTRAN CODE IN A VERIFICATION OF THE FINITE
* ELEMENT FORMULATION FOR THE TRANSIENT PROBLEM TO BE
* PURSUED IN THE NEXT PROGRAMING STEP.
* THE PROGRAM VERIFIES THE FINITE ELEMENT METHOD
* CODE LOGIC ON THREE POSSIBLE STATIC BEAM PROBLEM.
* (1) FIXED END WITH TWO ROLLER SUPPORTS, ONE AT THE CENTER
* AND A SECOND AT THE OPPOSITE END. THIS BEAM IS LOADED BY
* A CONCENTRATED MOMENT AT THE ROLLER SUPPORTED END.
* (2) AND (3) ARE CANTILEVER BEAM PROBLEMS, ONE LOADED BY A
* CONCENTRATED LOAD AT THE FREE END AND THE OTHER LOADED
* BY A CONCENTRATED MOMENT.
* THE PROGRAM IS NOT FLEXIBLE IN THAT IT REQUIRES EDITTING
* AS NOTED IN COMMENT LINES IN THE FOLLOWING SUBROUTINES
* DEPENDING ON WHICH OF THE (3) CASES IS BEING RUN. THE SOLE
* PURPOSE OF THIS PROGRAM IS TO VERIFY THE FEM FORMULATION,
* IT IS NOT INTENDED TO IMPRESS SOFTWARE ENGINEERS.
*
* (1) SUBROUTINE BC
* (2) SUBROUTINE OUTPUT
*****

```

C

```

*****
*                               VARIABLE IDENTIFICATION
*                               *
*****
* NEL - NUMBER OF ELEMENTS
* NSNP - NUMBER OF SYSTEM NODAL POINTS
* NDOF - NUMBER OF DEGREES OF FREEDOM
* E - MATERIAL MODULUS OF ELASTICITY
* GI - SECOND MOMENT OF THE BEAM CROSS-SECTION AREA
* BLGTH - BEAM STATIC LENGTH
* ELE - ELEMENT LENGTH
* BCM - EXTERNALLY APPLIED MOMENT AT FREE OR SIMPLY SUPPORTED
* END
* BCFORC- EXTERNALLY APPLIED FORCE AT FREE OR SIMPLY
* SUPPORTED END
* NDETRM - VARIABLE USED IN LOGIC STATEMENT FOR TYPE OF B.C.
* SLOPE - SLOPE AT FREE END OF CANTILEVER BEAM
* DEFLEC - DEFLECTION AT FREE END OF CANTILEVER BEAM
* FACTOR - SCALOR NON-DIMENSIONAL GROUP
*****

```

PARAMETER (N=70)

```

DIMENSION A(N,N),F(N)
DIMENSION WKAREA(6000)
OPEN(10, FILE='MATRIX OUTPUT')
CALL ZERO (A,F)
CALL DATA (NEL,NSNP,NDOF,E,GI,BLGTH,ELE,BCM,BCFORC)
CALL MATX (A,F,ELE,NEL,NDOF)
CALL BC (A,F,NDOF,NDETRM)
WRITE (10,*) ((A(J,K),K=1,NDOF),J=1,NDOF)
CALL LEQT2F(A,1,NDOF,N,F,0,WKAREA,IER)
CALL OUTPUT (NSNP,ELE,F,BCM,BLGTH,E,GI,NDETRM,NDOF,BCFORC)
STOP
END

C
C
C
C
ZERO ALL MATRICES
*****
SUBROUTINE ZERO (A,F)
PARAMETER (N=70)
DIMENSION A(N,N), F(N)
      DO 20 I=1,N
        F(I)=0.0
        DO 10 J=1,N
          A(I,J)=0.0
10      CONTINUE
20      CONTINUE
RETURN
END

C
C
C
C
INPUT DATA
*****
SUBROUTINE DATA (NEL,NSNP,NDOF,E,GI,BLGTH,ELE,BCM,BCFORC)

PRINT *, 'ENTER THE NO. OF ELEMENTS TO BE USED IN THE APPROX.'
READ *,NEL
WRITE(6,20) NEL
20  FORMAT (/2X,'NO. OF ELEMENTS IS',I5)
    NSNP=NEL+1
    WRITE(6,25) NSNP
25  FORMAT (/2X,'NO. OF SYSTEM NODAL POINTS IS',I5)
    NDOF=2*NSNP
    WRITE(6,26) NDOF
26  FORMAT (/2X,'NO. OF D.O.F. IS',I5)
    PRINT *, 'THE MODULUS OF ELASTICITY IS?'
    READ *,E
    WRITE(6,27) E
27  FORMAT (/2X,'MODULUS OF ELASTICITY IS', F10.1)
    PRINT *, 'THE SECOND MOMENT OF THE BEAM CROSS-SECTION AREA IS?'
    READ *,GI
    WRITE(6,28) GI
28  FORMAT (/2X,'THE SECOND MOMENT IS',F10.1)
    PRINT *, 'THE INITIAL LENGTH OF THE STATIC BEAM IS?'
    READ *, BLGTH
    WRITE(6,29) BLGTH
29  FORMAT (/2X,'THE BEAM LENGTH IS',F8.3)
    ELE=1.0/FLOAT(NEL)
    PRINT *, 'ENTER THE VALUE OF THE APPLIED MOMENT'
    READ *,BCM
    WRITE (6,30) BCM
30  FORMAT (/2X,'MOMENT=',F8.1)
    PRINT *, 'ENTER THE VALUE OF THE APPLIED FORCE'
    READ *,BCFORC
    WRITE (6,40) BCFORC
40  FORMAT (/2X,'FORCE=',F8.1)

C
RETURN
END

C
C
C
C
FILL LARGE A
*****
SUBROUTINE MATX (A,F,ELE,NEL,NDOF)
PARAMETER (N=70)

```

```

C      DIMENSION A(N,N),F(N)
C
C      CALCULATE LITTLE A MATRIX
C
C          A11=12.0/(ELE**3.0)
C          A12=6.0/(ELE**2.0)
C          A13=(-1.0)*A11
C          A14=A12
C          A21=A12
C          A22=4.0/ELE
C          A23=(-1.0)*A12
C          A24=2.0/ELE
C          A31=A13
C          A32=A23
C          A33=A11
C          A34=A23
C          A41=A14
C          A42=A24
C          A43=A34
C          A44=A22
C
C      FILL LARGE A MATRIX
C
C      L=2*NEL-1
C
C      DO 10 I=1,L,2
C
C          A(I,I)=A(I,I)+A11
C          A(I,I+1)=A(I,I+1)+A12
C          A(I,I+2)=A13
C          A(I,I+3)=A14
C
C          A(I+1,I)=A(I+1,I)+A21
C          A(I+1,I+1)=A(I+1,I+1)+A22
C          A(I+1,I+2)=A23
C          A(I+1,I+3)=A24
C
C          A(I+2,I)=A31
C          A(I+2,I+1)=A32
C          A(I+2,I+2)=A33
C          A(I+2,I+3)=A34
C
C          A(I+3,I)=A41
C          A(I+3,I+1)=A42
C          A(I+3,I+2)=A43
C          A(I+3,I+3)=A44
C
C 10  CONTINUE
C
C      RETURN
C      END
C
C      *****
C      THE FOLLOWING SUBROUTINE ALTERS THE GLOBAL MATRICES TO
C      IMPOSE THE BOUNDARY CONDITIONS
C
C      SUBROUTINE BC (A,F,NDOF,NDETRM)
C      PARAMETER(N=70)
C      DIMENSION A(N,N),F(N)
C      PRINT *, 'ENTER 1 FOR THE OVER DETERMINANT CASE OR'
C      PRINT *, '2 FOR THE FREE END CASE.'
C      READ *, NDETRM
C      IF (NDETRM .NE. 1) GOTO 20
C
C      AMEND A TO ACCOUNT FOR BOUNDARY CONDITIONS
C
C      CHANGE FIRST AND SECOND ROWS TO ACCOUNT FOR THE ESSENTIAL
C      BOUNDARY CONDITIONS AT THE FIXED END.
C
C      THE J-TH EQUATION IS THE EQUATION DESCRIBING DEFLECTION AT

```

```

C      THE LOCATION OF THE CENTER SUPPORT. IT IS REPLACED BY THE
C      ESSENTIAL BOUNDARY CONDITION ON DEFLECTION.
C
C      THE (NDOF-1)TH EQUATION IS THE EQUATION DESCRIBING THE
C      DEFLECTION AT THE ROLLER SUPPORTED END. THIS EQUATION
C      IS REPLACED BY THE ESSENTIAL B.C. ON DEFLECTION.
C
C      J=NDOF/2
C      DO 10 I=1,NDOF,1
C
C          A(1,I)=0.0
C          A(2,I)=0.0
C          A(J,I)=0.0
C          A(NDOF-1,I)=0.0
C
C      10  CONTINUE
C
C          A(1,1)=1.0
C          A(2,2)=1.0
C          A(J,J)=1.0
C          A(NDOF-1,NDOF-1)=1.0
C
C      GO TO 40
C      20  DO 30 I=1,NDOF,1
C          A(1,I)=0.0
C          A(2,I)=0.0
C      30  CONTINUE
C          A(1,1)=1.0
C          A(2,2)=1.0
C
C      ****POINT LOAD****
C      THIS LINE IS ACTIVATED FOR THE CANTILEVER BEAM LOADED
C      BY A CONCENTRATED LOAD CASE
C
C      F(NDOF-1)=1.0
C
C      ****POINT MOMENT****
C      THIS LINE MUST BE ACTIVATED FOR BOTH THE OVER DETERMINATE CASE
C      AND THE CANTILEVER BEAM WITH A CONCENTRATED MOMENT CASE
C
C      F(NDOF)=1.0
C
C      40  RETURN
C      END
C
C      FORMULATE OUTPUT
C      *****
C      THIS SUBROUTINE CALCULATES THE EXACT SOLUTION FOR THE
C      CANTILEVER BEAM CASES AS WELL AS PRINTS THE OUTPUT OF ALL
C      CASES.
C
C      SUBROUTINE OUTPUT (NSNP,ELE,F,BCM,BLGTH,E,GI,NDETRM,NDOF,BCFORC)
C      PARAMETER(N=70)
C      DIMENSION F(N)
C
C      ***POINT FORCE***
C      FACTOR=BCFORC*(BLGTH**2.0)/(E*GI)
C      DO 5 I=1,NDOF-1,2
C          F(I)=F(I)*BLGTH*FACTOR
C          F(I+1)=F(I+1)*FACTOR
C      5  CONTINUE
C
C      ***POINT MOMENT***
C      FACTOR=BLGTH*BCM/(E*GI)
C      DO 5 I=1,NDOF-1,2
C          F(I)=F(I)*BLGTH*FACTOR
C          F(I+1)=F(I+1)*FACTOR
C      5  CONTINUE
C
C      WRITE(*,30)
C      WRITE(*,40)

```

```

      IF (NDETRM .NE. 1) GOTO 15
      WRITE(*,50)
      J=1
      XLOC=0.0
      DO 10 I=1,NSNP,1
        WRITE(*,20) XLOC, F(J), F(J+1)
        XLOC=XLOC+ELE
        J=J+2
10     CONTINUE
      GO TO 80

C
C     ****POINT LOAD****
C     ACTIVATE FOR THE CANTILEVER-CONCENTRATE FORCE CASE
C
15    SLOPE=(BCFORC*(BLGTH**2.0))/(2.0*E*GI)
      DEFLEC=(BCFORC*(BLGTH**3.0))/(3.0*E*GI)

C
C     ****POINT MOMENT****
C     ACTIVATE FOR THE CANTILEVER BEAM CONCENTRATED MOMENT CASE
C
15    SLOPE=(BCM*BLGTH)/(E*GI)
      DEFLEC=(BCM*(BLGTH**2.0))/(2.0*E*GI)
C
      WRITE(*,60)
      WRITE(*,65)
      WRITE(*,70) DEFLEC,F(NDOF-1),SLOPE,F(NDOF)

20    FORMAT(2X,F8.3,3X,E12.4,3X,E12.4)
50    FORMAT(2X,' X-LOCATION',3X,'DEFLECTION',3X,'SLOPE')
60    FORMAT(1X,'          DEFLECTION AT B      ',',',',SLOPE AT B')
65    FORMAT(6X,'EXACT',11X,'FEM',11X,'EXACT',11X,'FEM')
70    FORMAT(1X,E12.4,3X,E12.4,3X,E12.4,3X,E12.4)
80    RETURN
      END

```


NO. OF ELEMENTS IS 8
 NO. OF SYSTEM NODAL POINTS IS 9
 NO. OF D.O.F. IS 18
 MODULUS OF ELASTICITY IS 30000000.0
 THE SECOND MOMENT IS 100.0
 THE BEAM LENGTH IS 100.000
 ENTER THE VALUE OF THE APPLIED MOMENT
 MOMENT = 0.0
 ENTER THE VALUE OF THE APPLIED FORCE
 FORCE= 1000.0
 ENTER 1 FOR THE OVER DETERMINANT CASE OR
 2 FOR THE FREE END CASE.

?
 2

DEFLECTION AT B		SLOPE AT B	
EXACT	FEM	EXACT	FEM
0.1111E+00	0.1111E+00	0.1667E-02	0.1667E-02

APPENDIX D **INTEGRATION BY PARTS**

The following is the detail of the integration by parts on the first term of Equation (54),

$$\int_0^1 Q(Q^T)_{\xi\xi\xi\xi} d\xi \delta \quad (137)$$

The first integration results in,

$$\begin{aligned} & \int_0^1 Q(Q^T)_{\xi\xi\xi\xi} d\xi \delta = \\ & Q(Q^T)_{\xi\xi\xi} \delta - \int_0^1 Q_{\xi}(Q^T)_{\xi\xi\xi} d\xi \delta \end{aligned} \quad (138)$$

A second integration performed on the integral in Equation (2) gives,

$$\begin{aligned} & - \int_0^1 Q_{\xi}(Q^T)_{\xi\xi\xi} d\xi \delta = \\ & - Q_{\xi}(Q^T)_{\xi\xi} \delta \Big|_0^1 + \int_0^1 Q_{\xi\xi}(Q^T)_{\xi\xi} d\xi \delta \end{aligned} \quad (139)$$

Combining Equations (1), (2), and (3) gives the symmetric operator and boundary terms below,

$$\int_0^1 \varrho (\varrho^r)_{\xi\xi\xi\xi} d\xi \delta =$$

$$\left[\varrho (\varrho^r)_{\xi\xi\xi} \delta - \varrho_{\xi} (\varrho^r)_{\xi\xi} \delta \right]_0^1 + \int_0^1 \varrho_{\xi\xi} (\varrho^r)_{\xi\xi} d\xi \delta \quad (140)$$

APPENDIX E

TRANSIENT BEHAVIOR OF A CANTILEVER BEAM FORTRAN CODE

```

*****
* MARK R DEVRIES LT USCG
* NAVAL POSTGRADUATE SCHOOL
* SEPTEMBER 1990
* THESIS
* MASTER OF SCIENCE IN MECHANICAL ENGINEERING
*
* TITLE:
* VIBRATION OF A CANTILEVER BEAM
* THAT SLIDES AXIALLY IN A FRICTIONLESS HOLE
*
* THE FOLLOWING FORTRAN CODE UTILIZES THE FINITE ELEMENT
* METHOD AND AN IMSL PACKAGE INTEGRATION SUBROUTINE DIVPAG
* TO SOLVE THE ABOVE PROBLEM. THE PROGRAM IS WRITTEN WITH
* NUMEROUS COMMENT LINES WHICH EXPLAIN THE CODING.
*****

*****
* VARIABLE IDENTIFICATION
*****
* NEL - NUMBER OF ELEMENTS
* NSNP - NUMBER OF SYSTEM NODAL POINTS
* NDOF - NUMBER OF DEGREES OF FREEDOM
* N,NN - DIMENSIONS OF MATRICES AS SPECIFIED IN DIMENSION
* STATEMENTS
* E - MATERIAL MODULUS OF ELASTICITY
* GI - SECOND MOMENT OF THE BEAM CROSS-SECTION AREA
* ELE - ELEMENT LENGTH
* ALPHA - LOCATION OF ELEMENT LEFT GNP
* PSIAVE - ESTIMATE OF PSI
* PSISQ - ESTIMATE OF PSI SQUARED
* TEND - VALUE OF TIME AT WHICH THE SOLUTION IS DESIRED
* NEQ - NO. OF FIRST ORDER DIFFERENTIAL EQUATIONS
* TIME - INDEPENDENT TIME VARIABLE
* DELTME - TOTAL TIME INCREMENT FOR ONE INTEGRATION STEP
* BETA - CONSTANT DETERMINED BY BEAM MATERIAL PROPERTIES ONLY
* RATE - LENGTH CHANGE PER UNIT TIME
* EXEE - THE GLOBAL NONDIMENSIONAL AXIS, THAT IS, (X/L)
* DELTA - THE VECTOR OF NONDIMENSIONAL NODE DEFLECTIONS
* AND SLOPES. MUST BE MULTIPLIED BY L(T) FOR
* ACTUAL DEFLECTIONS. SLOPES REMAIN THE SAME.
*
*****

INCLUDE 'COMMON FORTRAN'
DIMENSION DELTA(NN),PARAM(NPARAM),WKS(NN)
DIMENSION YPRIME(NN)
COMMON /WORKSP/ RWKSP

REAL RWKSP(6608)

EXTERNAL FCN
EXTERNAL FCNJ

```

```

OPEN(9, FILE='/MARK1 INPUT')
OPEN(10, FILE='/MARK3B OUTPUT')
OPEN(11, FILE='/DATA1 INPUT')
OPEN(12, FILE='/DATA2 INPUT')

CALL IWKIN(6608)
CALL ZERO (DELTA,PARAM)
CALL DATA
CALL MATX

PI = 3.141592654

C   DEFINITION OF PARAMETERS REQUIRED BY IMSL MATH LIBRARY ROUTINE
C   DIVPAG

IDO=1
NEQ=2*NDOF
TIME=TSTART
TOL=1.0E-4
PARAM(4)=2000000

C   PARAM(12) IS 1 FOR ADAMS METHOD AND 2 FOR GEAR (STIFF) METHOD

PARAM(12)=2
PARAM(13)=2
PARAM(19)=1
PARAM(20)=NN

C   INITIALIZE THE DEPENDENT VARIABLE ARRAY DELTA(NEQ).

** CAUTION: THE NONDIMENSIONAL VSTAR IS CONSTRUCTED HERE.
** TO OBTAIN THE ACTUAL INITIAL DISPLACEMENT CONFIGURATION, V,
** SUBSTITUTE THE NONDIMENSIONAL COORDINATE AXIS EXEE IN THE
** EXPRESSIONS BELOW BY (X/ZLINT) AND REPLACE VSTAR*ZLINT BY V

IF (ISTART.EQ.0) THEN
  IC=NDOF-1
  EXEE = 0.0
  WRITE(10,*) 'THE INITIAL TIME PRIOR TO INTEGRATION = ',TIME
  WRITE(10,*) 'THE INITIAL DELTA VECTOR IS'

  DO 10 I=1,IC,2
    PIOV2 = PI/2.
    C   DELTA(I) = 0.1 - 0.1*COS(PIOV2*EXEE)
    C   DELTA(I+1) = 0.1*PIOV2*SIN(PIOV2*EXEE)
    C   DELTA(I)=0.1*(EXEE**2.0)
    C   DELTA(I+1) = 0.2*EXEE

    WRITE (10,*) DELTA(I)
    WRITE (10,*) DELTA(I+1)
    EXEE = EXEE + ELE
10  CONTINUE

  ELSE
    READ(11,*) TSTART,ZL
    WRITE(10,*) 'RESTART TIME = ',TSTART, 'WITH LENGTH ',ZL
    READ(12,*) (DELTA(II),II=1,NEQ)
    WRITE(10,*) 'INITIAL DELTA IN RESTART FOLLOWS'
    WRITE(10,*) (DELTA(JJ),JJ=1,NEQ)
    TIME=TSTART

  END IF

IDO=1

CALL FORM(NEQ,TIME)

DO 1000 IEQ=1,NEQ
  YPRIME(IEQ)=0.0
  DO 900 IC=1,NEQ

```

```

          YPRIME(IEQ)=YPRIME(IEQ)+H(IEQ,IC)*DELTA(IC)
900    CONTINUE
1000  CONTINUE

C      WRITE(10,*) 'INITIAL YPRIME VECTOR PRIOR TO ENTRY TO DIVPAG'
C      WRITE (10,*) (YPRIME(IQ),IQ=1,NEQ)
      WRITE(10,*) ' '
      WRITE(10,*) ' '
      WRITE(10,*) 'IN INTEGRATION LOOP, TIME, LENGTH AND DELTA FOLLOWS'

      WORK = 0.0
      F1 = RHO*ZLINT*2.*ACC
      VEE = 6.*(DELTA(NDOF-3)-DELTA(NDOF-1))/ELE2
      & + 2.*(DELTA(NDOF-2)+2.*DELTA(NDOF))/ELE
      F2 = (E*GI)*(VEE**2)/(ZLINT**2)
      F3 = RHO*(-RATE*DELTA(NDOF) + ZLINT*DELTA(NEQ-1))*2
      FNEW = F1 + 0.5*(F2 - F3)
      ZL = ZLINT

      DO 30 IEND=1,NSTEP
      FOLD = FNEW
      ZLOLD = ZL
      TEND=TSTART+DELTME*FLOAT(IEND)/FLOAT(NSTEP)
      IF(TEND.GT.3.0) GO TO 35
      CALL DTIME(IHOUR,MINUTE,ISEC)
      C      IF(IHOUR.LT. 18 .AND. IHOUR.GE. 7) GO TO 35
      CALL DIVPAG (IDO,NEQ,FCN,FCNJ,G,TIME,TEND,TOL,PARAM,DELTA)
      IF (MOD(IEND,1).EQ.0) THEN
      ZL = ZLINT - RATE*TIME + ACC*(TIME**2)
      ZL2 = ZL**2
      ZLDOT = -RATE + 2.*ACC*TIME
      ZLDDOT = 2.*ACC
      C      ZL = 9. + 1.* COS( PI*TIME/1.5)
      C
      WRITE(10,*) ' '
      WRITE(10,*) ' '
      WRITE(10,*) 'TIME = ', TIME, 'LENGTH = ', ZL
      WRITE(10,*) ' '
      WRITE(10,*) 'DELTA FOLLOWS'
      WRITE(10,*) (DELTA(IQ),IQ=1,NEQ)
      C
      ZMOM = (E*GI/ZL)*((6./ELE2)*(DELTA(3)-DELTA(1))
      & -(2./ELE)*(DELTA(4)+2.*DELTA(2)))
      SHEAR = (E*GI/ZL2)*((12./ELE3)*(DELTA(1)-DELTA(3))
      & +(6./ELE2)*(DELTA(2)+DELTA(4)))
      WRITE(10,*) ' '
      WRITE(10,*) 'MOMENT = ', ZMOM, 'SHEAR = ', SHEAR
      END IF

      F1 = RHO*ZLINT*2.*ACC
      VEE = 6.*(DELTA(NDOF-3)-DELTA(NDOF-1))/ELE2
      & + 2.*(DELTA(NDOF-2)+2.*DELTA(NDOF))/ELE
      F2 = (E*GI)*(VEE**2)/ZL2
      F3 = RHO*(-ZLDOT*DELTA(NDOF) + ZL*DELTA(NEQ-1))*2
      FNEW = F1 + 0.5*(F2 - F3)

      DELWORK = 0.5*(FNEW + FOLD)*(ZL - ZLOLD)
      WORK = WORK + DELWORK
      WRITE(10,*) 'ZLDOT = ', ZLDOT, 'ZLDDOT = ', ZLDDOT
      WRITE(10,*) 'OLD F = ', FOLD, 'NEW F = ', FNEW
      WRITE(10,*) 'WORK = ', WORK

      CALL FORM(NEQ,TIME)

30    CONTINUE
35    CONTINUE

      IDO=3
      CALL DIVPAG (IDO,NEQ,FCN,FCNJ,G,TIME,TEND,TOL,PARAM,DELTA)

      STOP
      END

```

```

C      ZERO ALL MATRICES
      *****
      SUBROUTINE ZERO (DELTA,PARAM)

      INCLUDE 'COMMON FORTRAN'
      DIMENSION DELTA(NN),PARAM(NPARAM)

      DO 20 I=1,N
        DO 10 J=1,N
          A(I,J)=0.0
          B(I,J)=0.0
          C(I,J)=0.0
          D(I,J)=0.0
          R(I,J)=0.0
10      CONTINUE
20      CONTINUE

      DO 40 I=1,NN
        DELTA(I)=0.0
        DO 35 J=1,NN
          G(I,J)=0.0
          H(I,J)=0.0
35      CONTINUE
40      CONTINUE

      DO 50 I=1,NPARAM
        PARAM(I)=0.0
50      CONTINUE

      RETURN
      END

C      INPUT DATA
      *****
      SUBROUTINE DATA

      INCLUDE 'COMMON FORTRAN'

      READ (9,*) NEL,E,GI,RHO,NSTEP,ISTART,TSTART,ZLINT,DELTIME,RATE,ACC

      WRITE(6,*) 'THE NUMBER OF ELEMENTS IS ', NEL

      NSNP=NEL+1
      NDOF=2*NSNP

      WRITE(6,*) 'THE NUMBER OF SYSTEM NODAL POINTS IS ', NSNP

      WRITE(6,*) 'THE NUMBER OF DEGREES OF FREEDOM IS ', NDOF
      WRITE(6,*) 'THE MODULUS OF ELASTICITY IS ', E
      WRITE(6,*) 'THE MOMENT OF INERTIA IS ', GI
      WRITE(6,*) 'THE MASS PER UNIT LENGTH IS ', RHO

      ELE=1.0/FLOAT(NEL)
      ELE2 = ELE**2
      ELE3 = ELE**3
      BETA=RHO/(E*GI)
      WRITE(6,*) 'THE VALUE OF BETA IS ', BETA

      WRITE(6,*) 'THE NUMBER OF INTEGRATION STEPS IS ', NSTEP
      WRITE(6,*) 'ISTART IS 1 FOR RESTART; HERE IT IS ', ISTART
      WRITE(6,*) 'THE INITIAL LENGTH IS ', ZLINT
      WRITE(6,*) 'RATE OF AXIAL MOTION IS ', RATE

      RETURN
      END

C      FILL LARGE A
C      *****
      SUBROUTINE MATX

```

INCLUDE 'COMMON FORTRAN'

C CALCULATE LITTLE A MATRIX

A11=12.0/(ELE**3.0)
A12=6.0/(ELE**2.0)
A13=(-1.0)*A11
A14=A12
A21=A12
A22=4.0/ELE
A23=(-1.0)*A12
A24=2.0/ELE
A31=A13
A32=A23
A33=A11
A34=A23
A41=A14
A42=A24
A43=A34
A44=A22

C CALCULATE THE ELEMENTAL B MATRIX

B11=(-6.0)/(5.0*ELE)
B12=-1.1
B13=(-1.0)*B11
B14=-.1
B21=B14
B22=(-2.0*ELE)/15.0
B23=.1
B24=ELE/30.0
B31=B13
B32=B23
B33=B11
B34=1.1
B41=B21
B42=B24
B43=.1
B44=B22

C
C CALCULATE THE ELEMENTAL C MATRIX

C11=-.5
C12=ELE/10.0
C13=.5
C14=(-.1)*ELE
C21=C14
C22=0.0
C23=C12
C24=(ELE**2)/(-60.0)
C31=C11
C32=C21
C33=C13
C34=C12
C41=C12
C42=(-1.0)*C24
C43=C32
C44=C22

C
C
C CALCULATE THE ELEMENTAL D MATRIX

D11=13.0*ELE/35.0
D12=(11.0/210.0)*(ELE**2.0)
D13=9.0*ELE/70.0
D14=(-13.0/420.0)*(ELE**2)
D21=D12
D22=(ELE**3.0)/(105.)
D23=(13.0*ELE**2)/420.
D24=-(ELE**3.0)/(140.0)
D31=D13
D32=D23


```

D33=D11
D34=(-11.0*ELE**2)/210.
D41=D14
D42=D24
D43=D34
D44=D22

```

C FILL THE GLOBAL A,B,C, AND D MATRICES

```
LNEL = 2*NEL-1
```

```
DO 10 I=1, LNEL, 2
```

```
ALPHA=0.0
```

```
PSIAVE=ALPHA+(ELE/2.0)
PSISQ=PSIAVE**2
```

```

A(I,I)=A(I,I)+A11
A(I,I+1)=A(I,I+1)+A12
A(I,I+2)=A13
A(I,I+3)=A14

```

```

A(I+1,I)=A(I+1,I)+A21
A(I+1,I+1)=A(I+1,I+1)+A22
A(I+1,I+2)=A23
A(I+1,I+3)=A24

```

```

A(I+2,I)=A31
A(I+2,I+1)=A32
A(I+2,I+2)=A33
A(I+2,I+3)=A34

```

```

A(I+3,I)=A41
A(I+3,I+1)=A42
A(I+3,I+2)=A43
A(I+3,I+3)=A44

```

```

B(I,I)=B(I,I)+(B11*PSISQ)
B(I,I+1)=B(I,I+1)+(B12*PSISQ)
B(I,I+2)=B13*PSISQ
B(I,I+3)=B14*PSISQ

```

```

B(I+1,I)=B(I+1,I)+(B21*PSISQ)
B(I+1,I+1)=B(I+1,I+1)+(B22*PSISQ)
B(I+1,I+2)=B23*PSISQ
B(I+1,I+3)=B24*PSISQ

```

```

B(I+2,I)=B31*PSISQ
B(I+2,I+1)=B32*PSISQ
B(I+2,I+2)=B33*PSISQ
B(I+2,I+3)=B34*PSISQ

```

```

B(I+3,I)=B41*PSISQ
B(I+3,I+1)=B42*PSISQ
B(I+3,I+2)=B43*PSISQ
B(I+3,I+3)=B44*PSISQ

```

```

C(I,I)=C(I,I)+(C11*PSIAVE)
C(I,I+1)=C(I,I+1)+(C12*PSIAVE)
C(I,I+2)=C13*PSIAVE
C(I,I+3)=C14*PSIAVE

```

```

C(I+1,I)=C(I+1,I)+(C21*PSIAVE)
C(I+1,I+1)=C(I+1,I+1)+(C22*PSIAVE)
C(I+1,I+2)=C23*PSIAVE
C(I+1,I+3)=C24*PSIAVE

```

```

C(I+2,I)=C31*PSIAVE
C(I+2,I+1)=C32*PSIAVE
C(I+2,I+2)=C33*PSIAVE

```

```

      C(I+2,I+3)=C34*PSIAVE
      C(I+3,I)=C41*PSIAVE
      C(I+3,I+1)=C42*PSIAVE
      C(I+3,I+2)=C43*PSIAVE
      C(I+3,I+3)=C44*PSIAVE

      D(I,I)=D(I,I)+D11
      D(I,I+1)=D(I,I+1)+D12
      D(I,I+2)=D13
      D(I,I+3)=D14

      D(I+1,I)=D(I+1,I)+D21
      D(I+1,I+1)=D(I+1,I+1)+D22
      D(I+1,I+2)=D23
      D(I+1,I+3)=D24

      D(I+2,I)=D31
      D(I+2,I+1)=D32
      D(I+2,I+2)=D33
      D(I+2,I+3)=D34

      D(I+3,I)=D41
      D(I+3,I+1)=D42
      D(I+3,I+2)=D43
      D(I+3,I+3)=D44

      ALPHA=ALPHA+ELE

10  CONTINUE

      RETURN
      END

*****
      SUBROUTINE FORM(NEQ,TIME)
      INCLUDE 'COMMON FORTRAN'

      ZL = ZLINT - RATE*TIME + ACC*(TIME**2)
      ZLDOT = -RATE + 2.*ACC*TIME
      ZLDDOT = 2.*ACC
      PI = 3.141592654
      PARAM = PI/1.5
C     ZL = 9. + 1.* COS( PARAM*TIME)
C     ZLDOT = -(PARAM)*SIN(PARAM*TIME)
C     ZLDDOT = -(PARAM**2)*COS(PARAM*TIME)
      ACCOEFF=(-1.0)/((ZL**4)*BETA)
      EOCOEFF= -((ZLDOT/ZL)**2)
      CCOEFF= -(2.*(ZLDOT/ZL)**2) + ZLDDOT

      DO 20 I=1,NDOF
        DO 15 J=1,NDOF
          R(I,J)= A(I,J)*ACOEFF + B(I,J)*BCOEFF + C(I,J)*CCOEFF
          CC(I,J)= -2.*BETA*(ZLDOT/ZL)*C(I,J)
15        CONTINUE
20      CONTINUE

C     REDUCE SYSTEM OF EQUATIONS FROM SECOND TO FIRST O.D.E.

      DO 100 I=1,NDOF
        G(I,I)=1.0
100    CONTINUE

      DO 300 I=1,NDOF
        K=I+NDOF
        DO 200 J=1,NDOF
          LL=J+NDOF
          G(K,LL)=D(I,J)
200      CONTINUE
300    CONTINUE

```

```

      DO 400 I=1,NDOF
        II=I+NDOF
        H(I,II)=1.0
400    CONTINUE

      DO 600 I=1,NDOF
        K=I+NDOF
        DO 500 J=1,NDOF
          H(K,J)=R(I,J)
500      CONTINUE
600    CONTINUE

      DO 700 I=1,NDOF
        II=I+NDOF
        DO 650 J=1,NDOF
          JJ=J+NDOF
          H(II,JJ) = CC(I,J)
650    CONTINUE
700    CONTINUE

C      IMPOSE FIXED END BOUNDARY CONDITIONS

      DO 800 J=1,2
        DO 750 I=1,NEQ
          G(J+NDOF,I)=0.0
          H(J,I)=0.0
          H(J+NDOF,I)=0.0
750      CONTINUE
800    CONTINUE

      G(NDOF+1,NDOF+1)=1.0
      G(NDOF+2,NDOF+2)=1.0

      RETURN
      END

      *****

      SUBROUTINE FCN (NEQ,TIME,DELTA,YPRIME)

      INCLUDE 'COMMON FORTRAN'
      DIMENSION YPRIME(NEQ),DELTA(NEQ)
      REAL L

      DELTA(1) = 0.0
      DELTA(2) = 0.0
      DELTA(NDOF+1) = 0.0
      DELTA(NDOF+2) = 0.0

C      FORM YPRIME

      DO 1000 IEQ=1,NEQ
        YPRIME(IEQ)=0.0
        DO 900 IC=1,NEQ
          YPRIME(IEQ)=YPRIME(IEQ)+H(IEQ,IC)*DELTA(IC)
900      CONTINUE
1000    CONTINUE

      RETURN
      END

      FUNCTION FCNJ(NEQ, TIME, DELTA, PD)
      REAL TIME, DELTA(NEQ), PD(*)
      FCNJ=0.0
      RETURN
      END

```

LIST OF REFERENCES

1. Naval Postgraduate School Report NPS-69-79-009, Vibration of a Cantilever Beam That Slides Axially in a Rigid Frictionless Hole, by A. Boresi and D. Salinas, September 1979.
2. Bellman, R., and Kababa, R., Quasilinearization, and Nonlinear Boundary - Value Problems, American Elsevier Publishing Co., 1965.
3. Crandall, S.H., Karnopp, D.C., Kurtz Jr., E.F., and Pudmore-Brown, D.C., Dynamics of Mechanical and Electromechanical Systems, p. 344-347, McGraw-Hill Book Co., 1968.